Detectors for X-ray imaging

Pr Christian MOREL, PhD

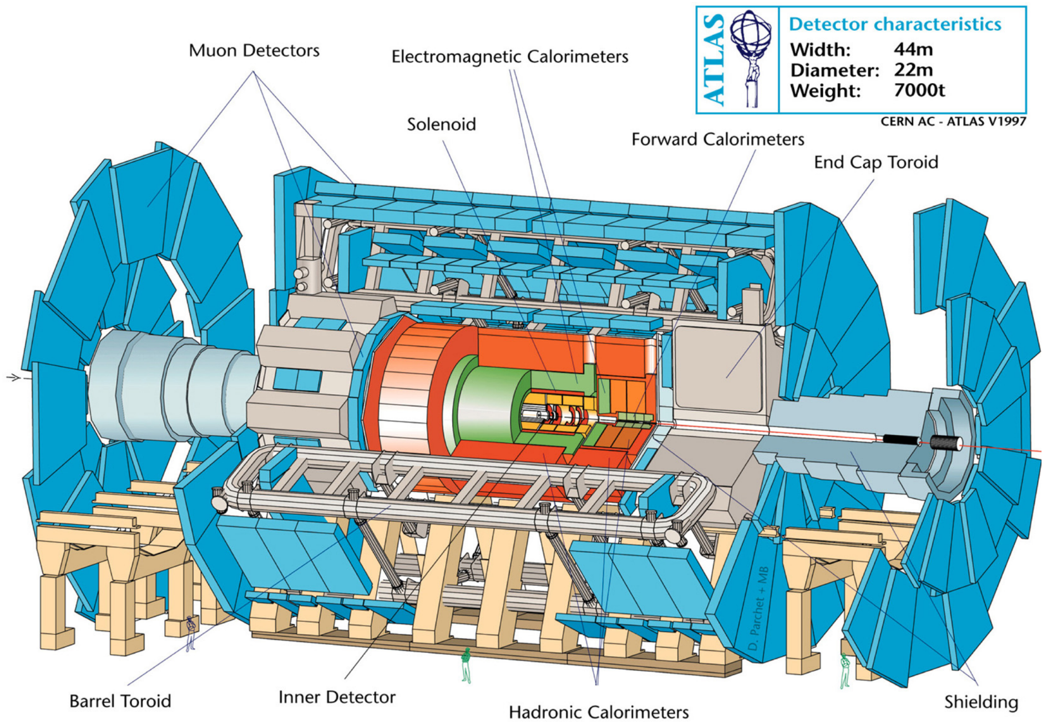

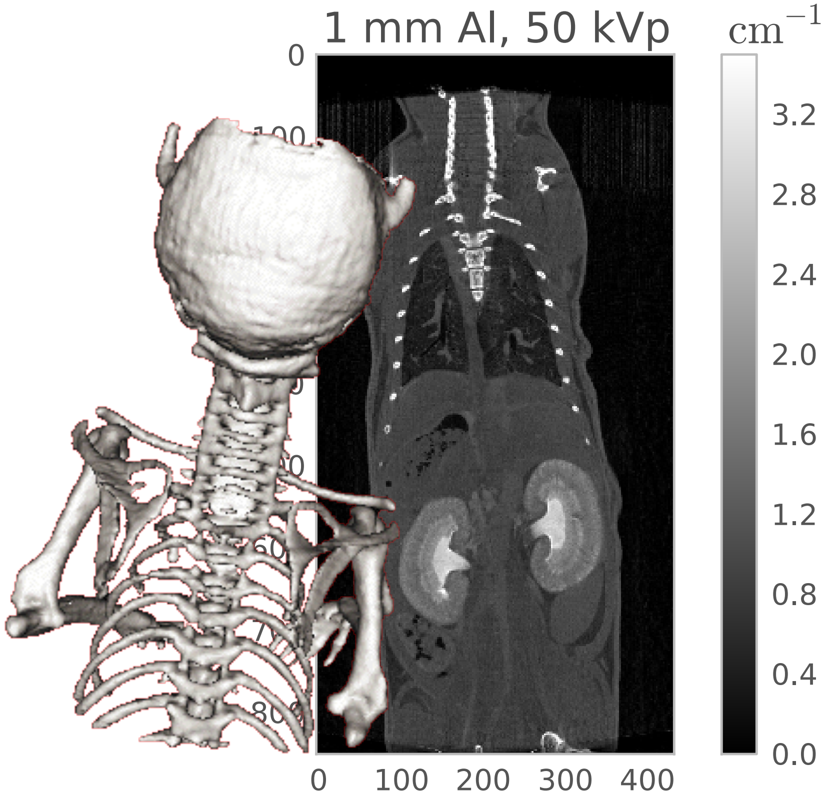

Ecole d'été France Excellence, Marseille, 1-11 Jul 2019

Aix*Marseille université
cnrs IN2P3 Les deux infinis
CENTRE DE PHYSIQUE DES PARTICULES DE MARSEILLE CPPM

Discovery of X-rays (1895)

Wilhelm Roentgen (1845-1923)
Nobel Prize in Physics (1901)

22 Dec 1895 – published in the New York Times on 16 Jan 1896

Development of radiology (roentgenology)

Hôpital Tenon (Paris, 1897)
Antoine Béclère (1858–1939)

Radiological Renault «Petite Curie» (1916)
Marie Curie (1867-1934)

Development of Computerized Tomography (CT)

Rediscovery of the Radon solution for reconstruction from projections (Cape Town, 1963)
Allan McLoed Cormack (1924-1998)

Development of the first CT scanner at EMI (London, 1972)
Sir Godfrey Newbold Hounsfield (1919-2004)

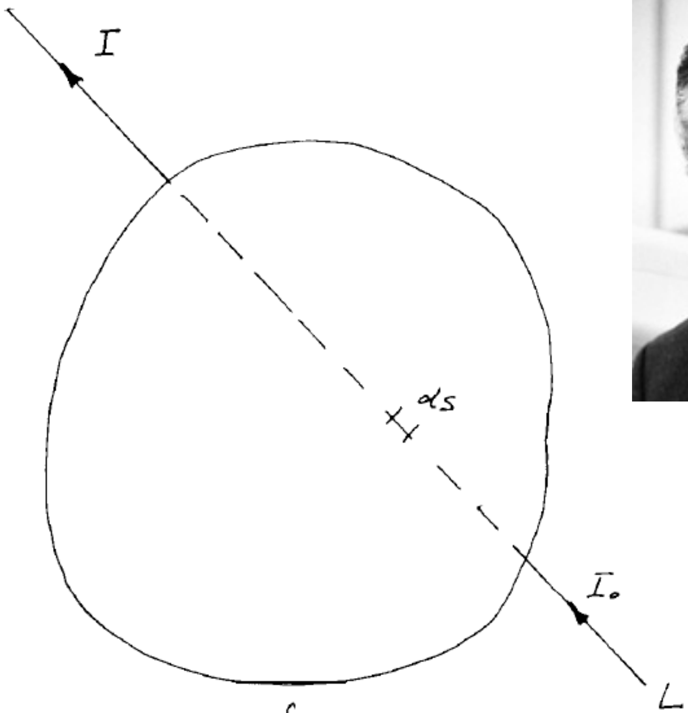

$$I = I_0 e^{-\int_L f\,ds}$$

300 detectors
Scan time 2 - 4 seconds

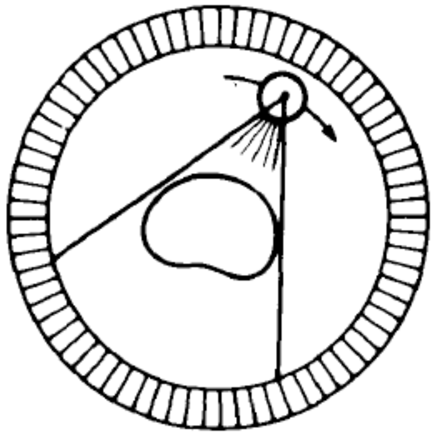

700 stationary detectors
Scan time 2 - 4 seconds

Nobel Prize in Medicine (1979)

Computerized Tomography (CT)

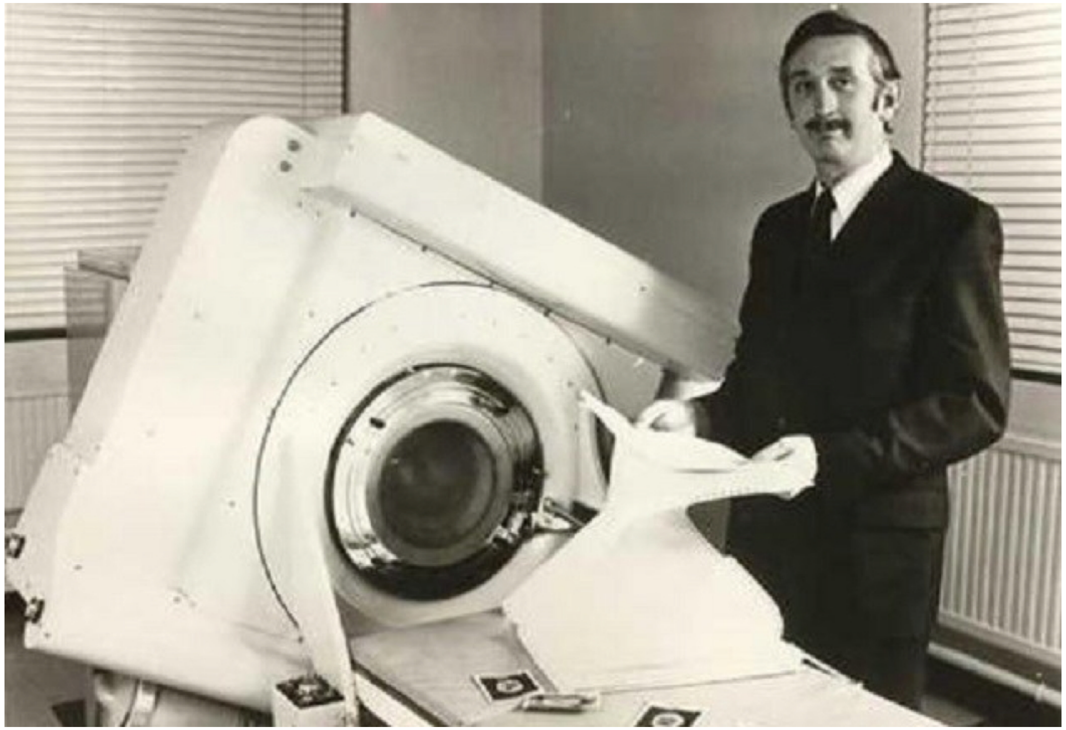

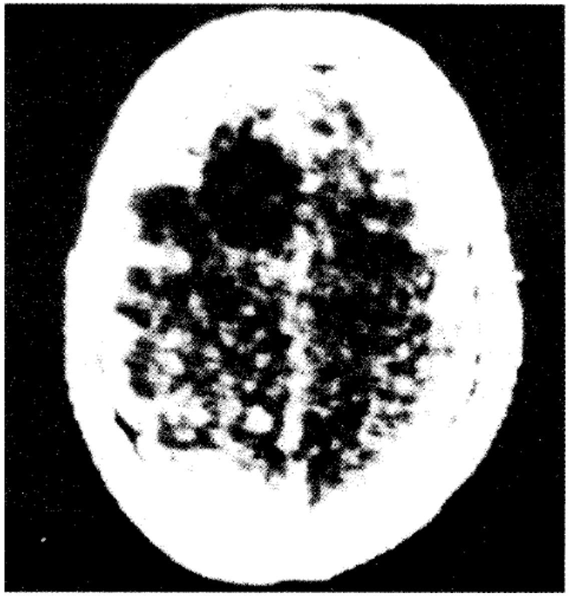

G. Hounsfield, J. Ambrose
(Atkinson Morley Hospital, London, 1/10/1971)

X-ray CT scanner

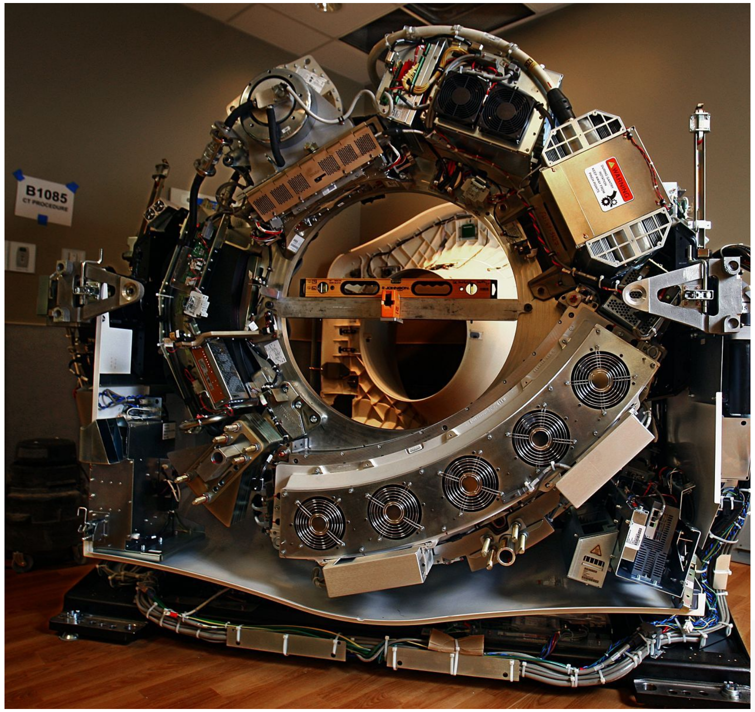

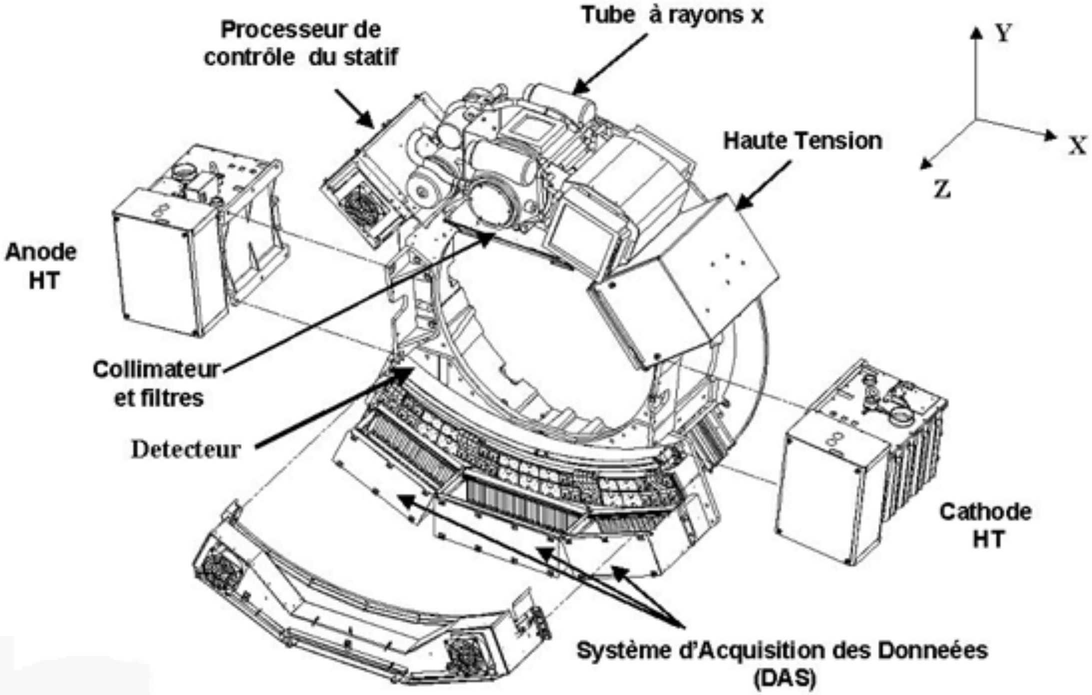

Diagnostic procedure	*Typical effective dose (mSv)*	*Equiv. no. of CXR*	*Approx. equiv. period of background radiation*
CXR	0.02	1	3 days
CT head	2.0	100	10 months
CT chest	8	400	3.6 years
CT abdomen/pelvis	10	500	4.5 years

UK average background radiation = 2.2 mSv per year; regional averages range from 1.5 to 7.5 mSv per year.

Transmission tomography

Monochromatic case

$$I = I_0 \exp[-\int_{t_1}^{t_2} \mu_E(t)\,dt]$$

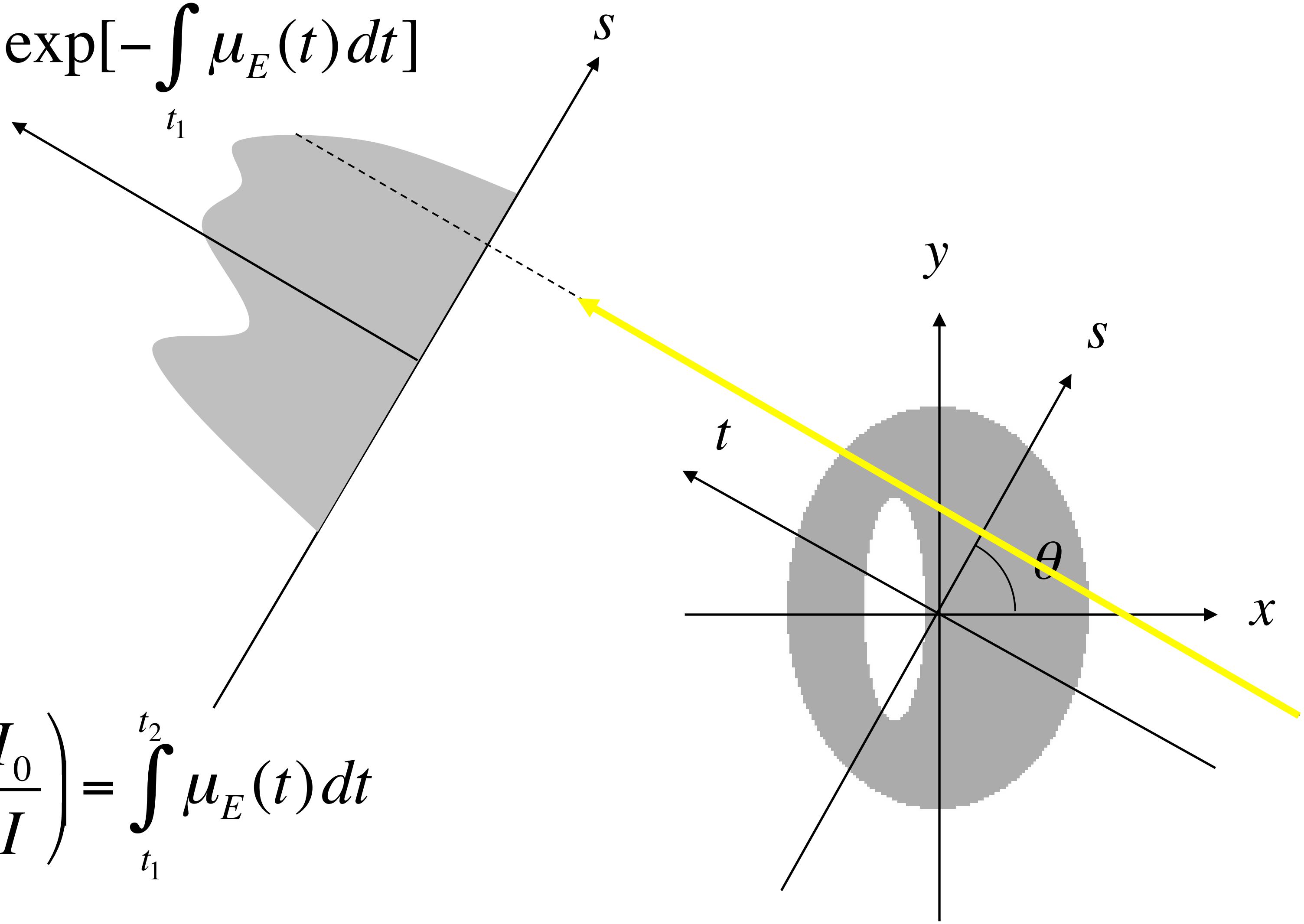

$$\ln\left(\frac{I_0}{I}\right) = \int_{t_1}^{t_2} \mu_E(t)\,dt$$

Transmission tomography

Polychromatic case

$$I_0 = \int_0^{\infty} I_0(E)\,dE$$

$$I = \int_0^{\infty} I_0(E)\exp[-\int_{t_1}^{t_2} \mu_E(t)\,dt]\,dE$$

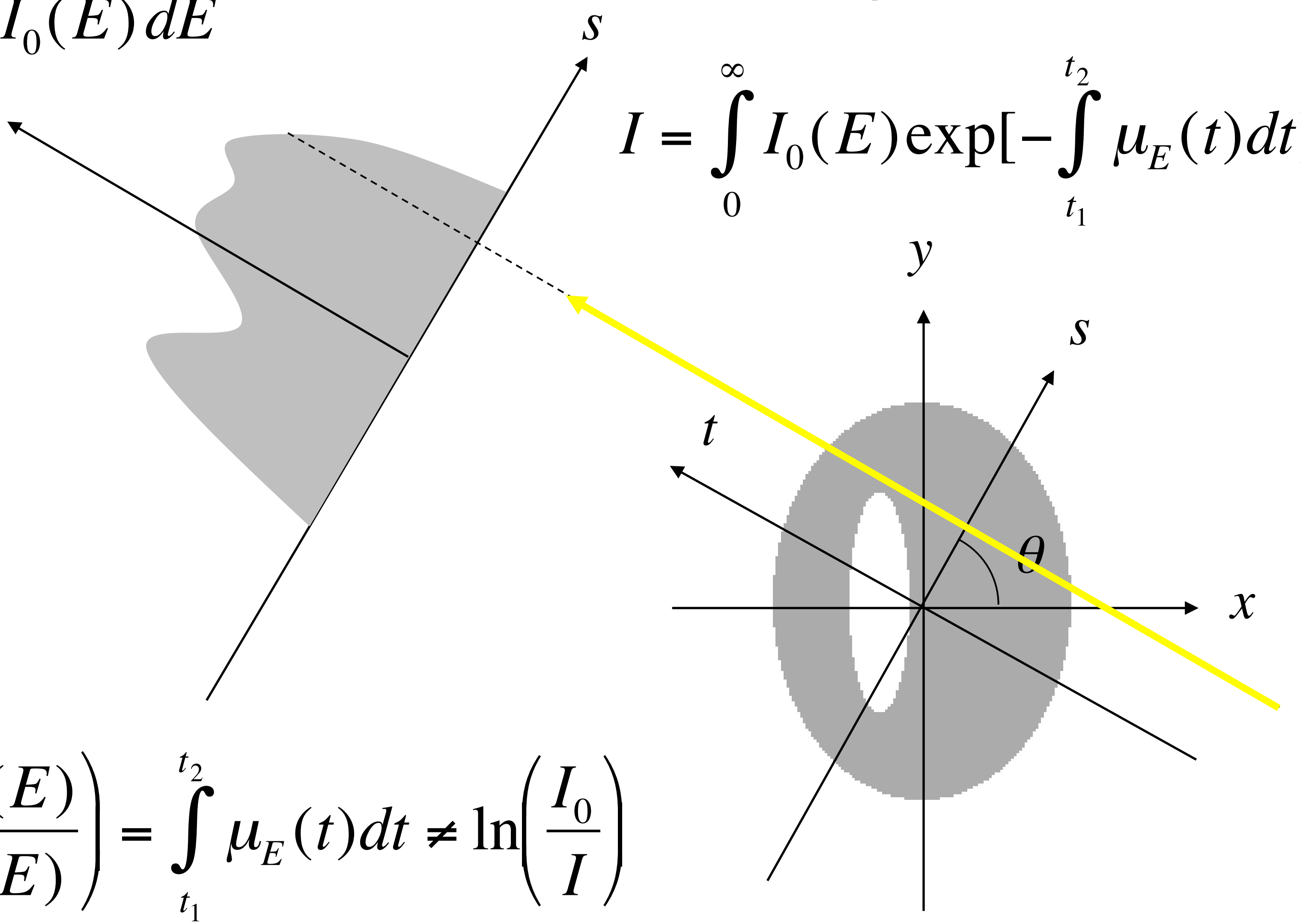

$$\ln\left(\frac{I_0(E)}{I(E)}\right) = \int_{t_1}^{t_2} \mu_E(t)\,dt \neq \ln\left(\frac{I_0}{I}\right)$$

Transmission tomography

Polychromatic case -> beam hardening

$$I_0 = \int_0^\infty I_0(E)\,dE$$

$$I = \int_0^\infty I_0(E)\exp[-\int_{t_1}^{t_2} \mu_E(t)\,dt]\,dE$$

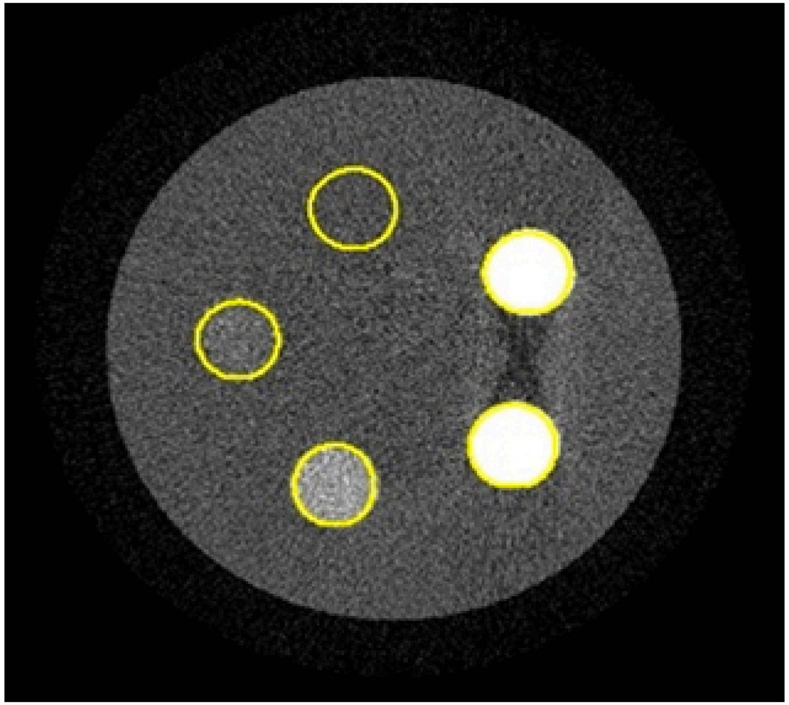

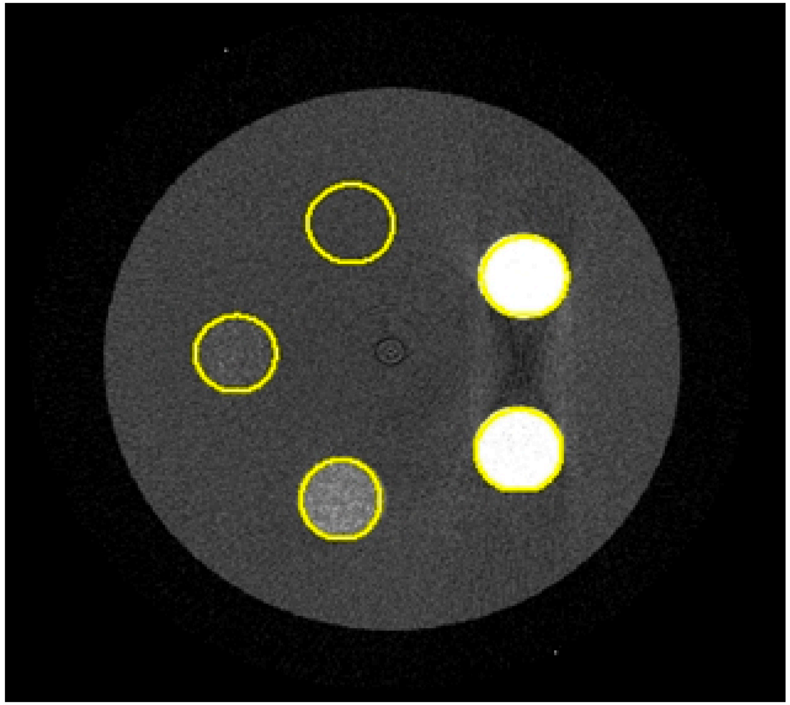

$$\ln\left(\frac{I_0(E)}{I(E)}\right) = \int_{t_1}^{t_2} \mu_E(t)\,dt \neq \ln\left(\frac{I_0}{I}\right)$$

Hounsfield Units (HU)

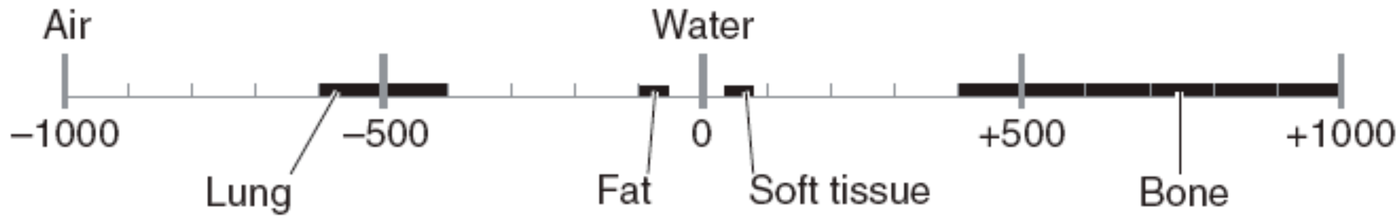

Bone	+400 → +1000
Soft tissue	+40 → +80
Water	0
Fat	–60 → –100
Lung	–400 → –600
Air	–1000

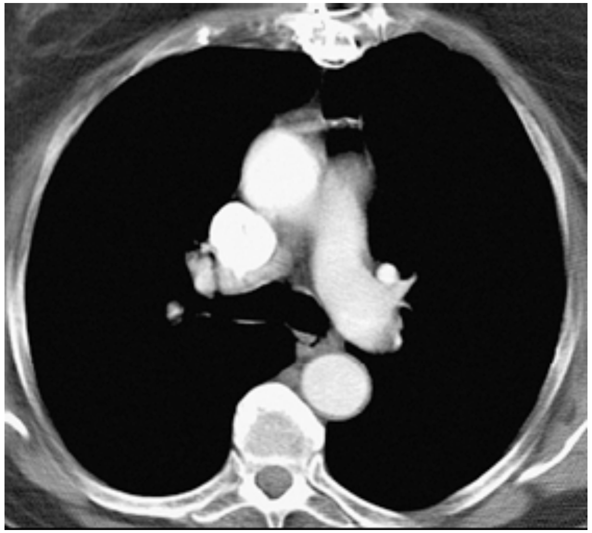

[40-390] HU

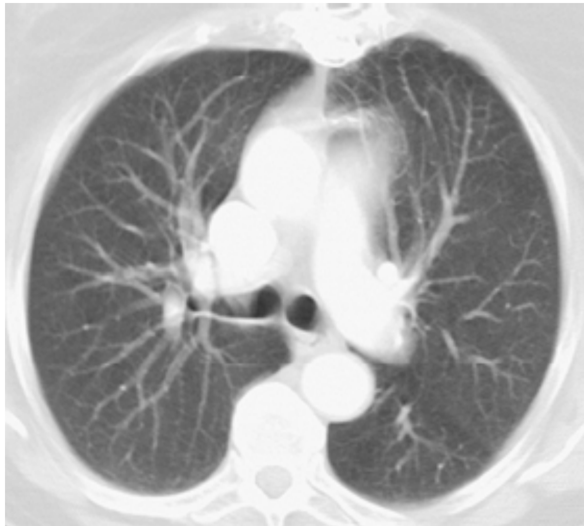

[−600-900] HU

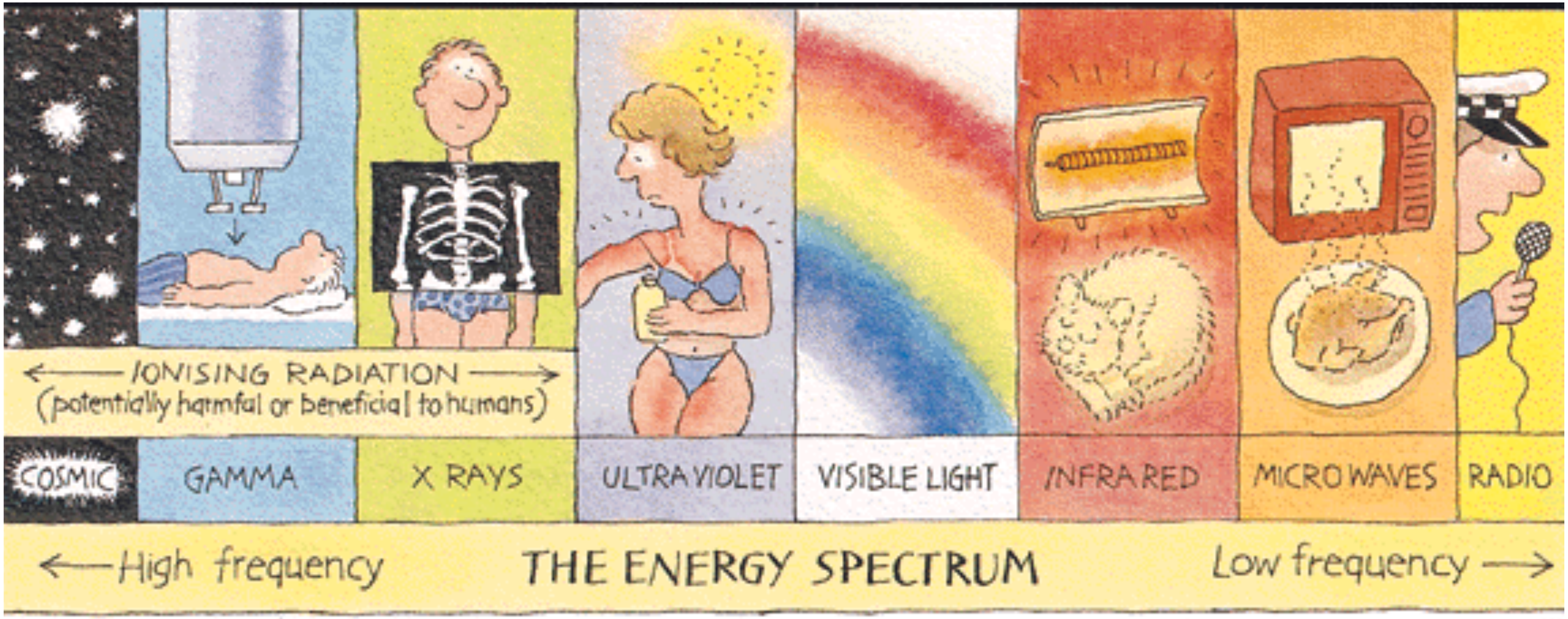
IONISING RADIATION
(potentially harmful or beneficial to humans)
COSMIC
GAMMA
X RAYS
ULTRAVIOLET
VISIBLE LIGHT
INFRARED
MICRO WAVES
RADIO
High frequency
THE ENERGY SPECTRUM
Low frequency

EM spectrum

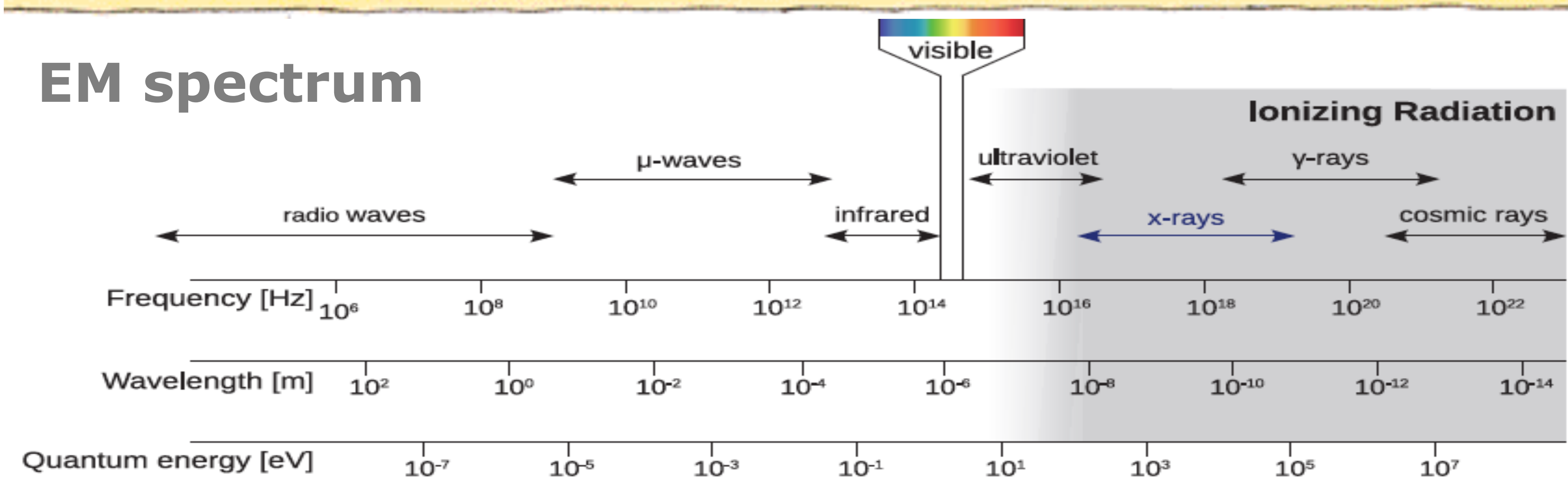
visible
Ionizing Radiation
μ-waves
ultraviolet
γ-rays
radio waves
infrared
x-rays
cosmic rays
Frequency [Hz] 10^{6} 10^{8} 10^{10} 10^{12} 10^{14} 10^{16} 10^{18} 10^{20} 10^{22}
Wavelength [m] 10^{2} 10^{0} 10^{-2} 10^{-4} 10^{-6} 10^{-8} 10^{-10} 10^{-12} 10^{-14}
Quantum energy [eV] 10^{-7} 10^{-5} 10^{-3} 10^{-1} 10^{1} 10^{3} 10^{5} 10^{7}

X-ray detection paradigm

Indirect detection

Scintillator or phosphor screen
Radiation converted to light

Photodetector (*e.g.* PMT, photodiode, CCD camera or CMOS pixel)
Light converted to electric signal

Image

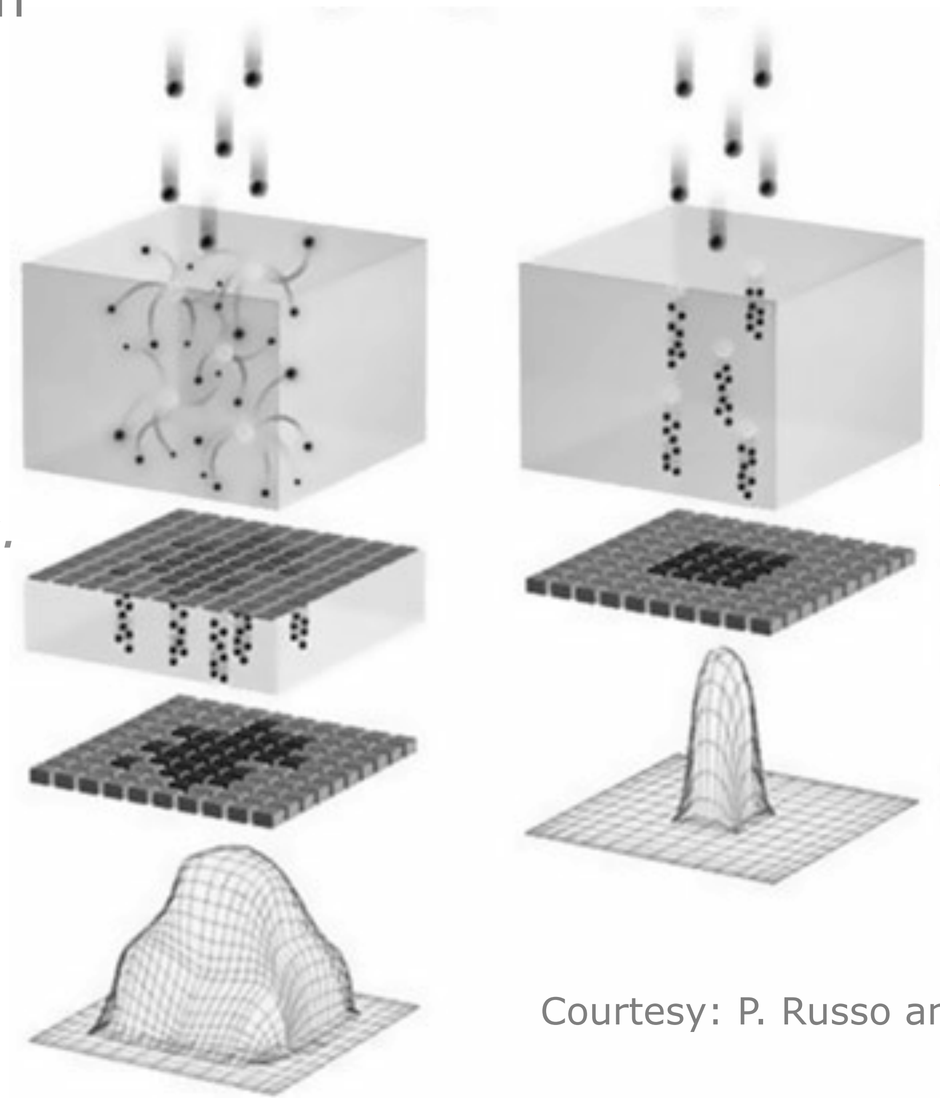

Direct detection

Gaz (*e.g.* Xe) or semiconductor (*e.g.* Si, CdTe, AsGa)
radiation converted to electric signal

Readout electronic circuit

Image

Courtesy: P. Russo and A. Del Guerra, INFN

Charge integration detectors

Converter

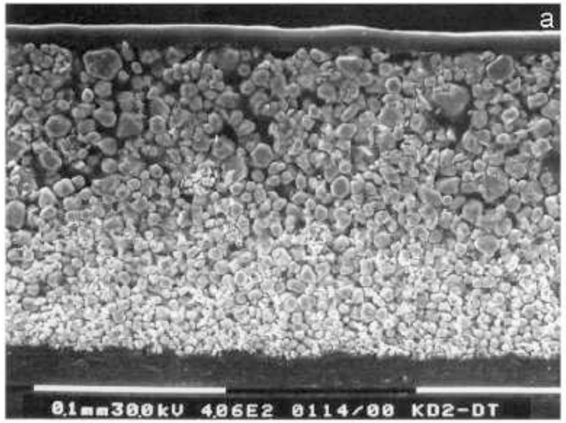

Gadolinium oxysulfide
(GOS or Gadox, Gd_2O_2S)

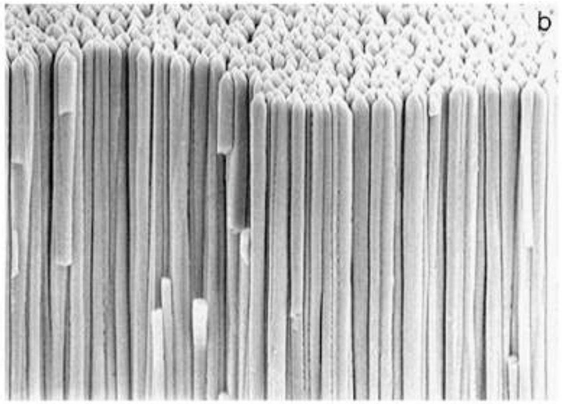

Cesium iodide (CsI)

Photodetector

Charged Couple Device (CCD) camera

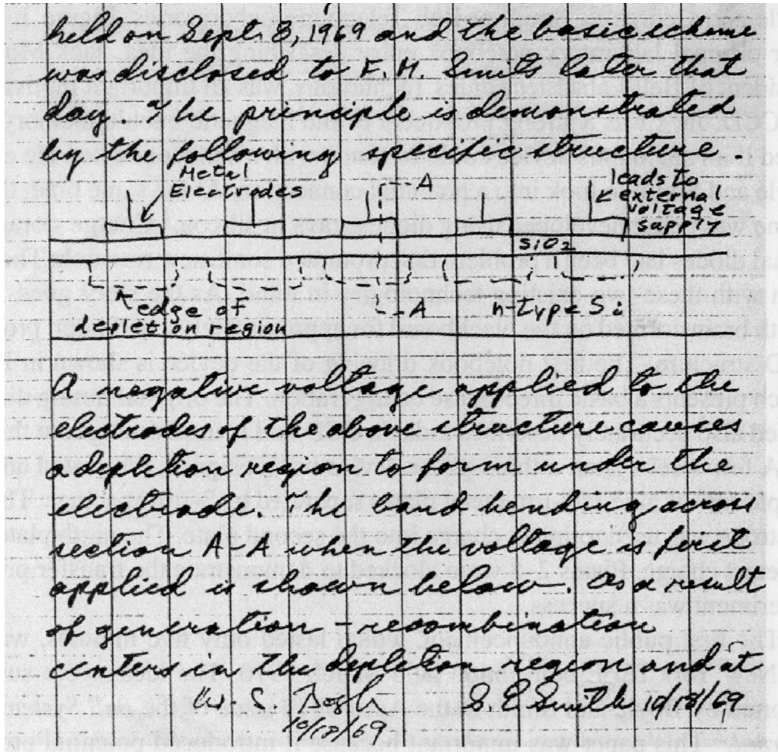
held on Sept. 8, 1969 and the basic scheme
was disclosed to F. H. Smits later that
day. The principle is demonstrated
by the following specific structure.

A negative voltage applied to the
electrodes of the above structure causes
a depletion region to form under the
electrode. The band bending across
section A-A when the voltage is first
applied is shown below. As a result
of generation-recombination
centers in the depletion region and at

W. S. Boyle 10/18/69 G. E. Smith 10/18/69

W.S. Boyle and G.E. Smith (Bell Labs, 1969)
Nobel Prize in Physics (2009)

Complementary Metal-Oxyde Semiconductor
(CMOS) pixel

Trajectography at the LHC ATLAS experiment

Thousands of particles every 20 ns

Reconstruct every track

2D detectors

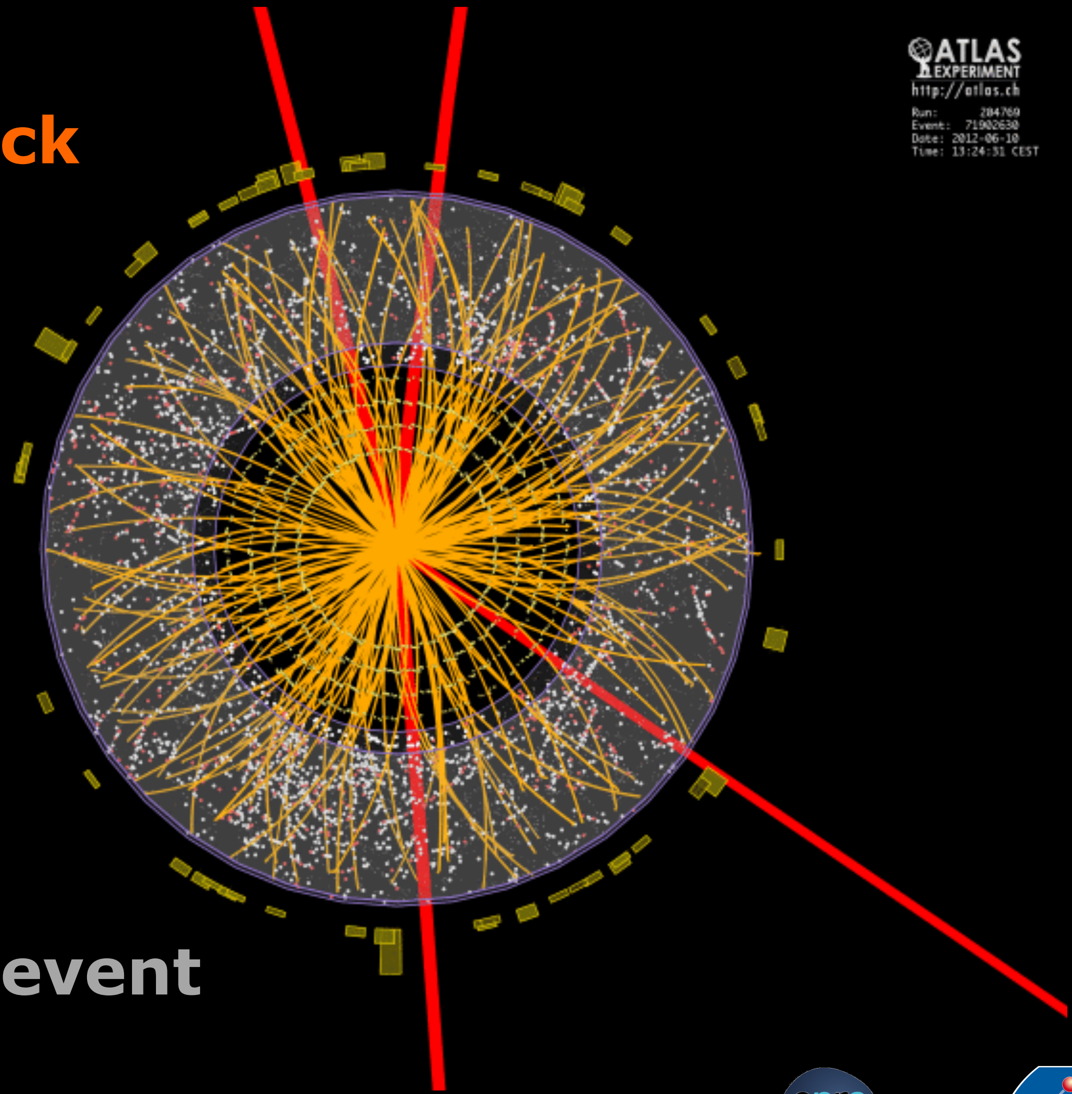

Higgs event

CNRS IN2P3 Les deux infinis

CENTRE DE PHYSIQUE DES PARTICULES DE MARSEILLE CPPM

Hybrid Pixels: from LHC micro-vertex detectors to photon counting CT

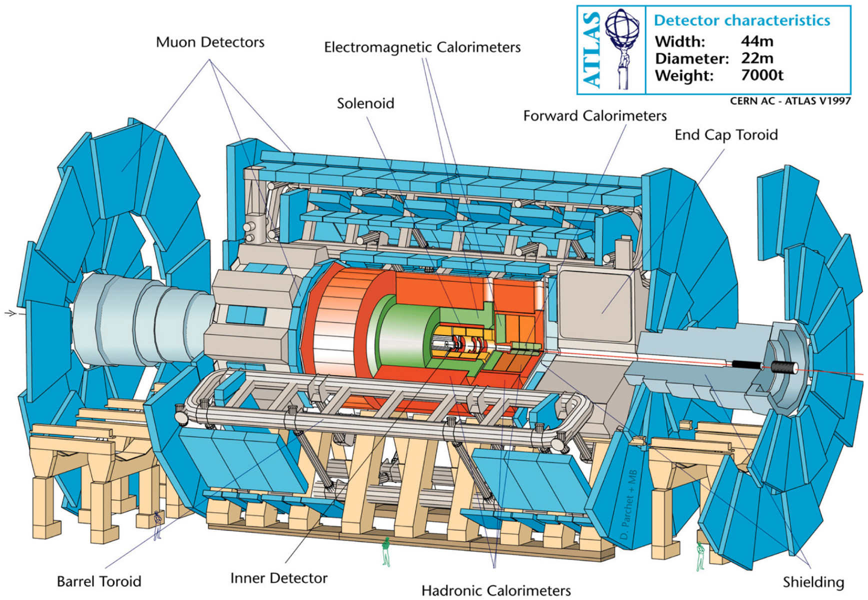

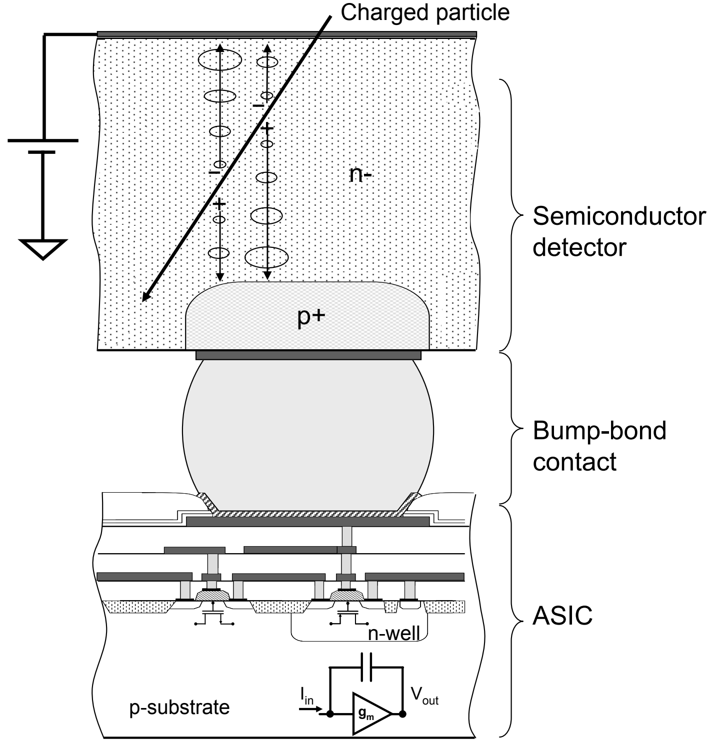

- Noise suppression
- Energy selection
- Very high dynamics

Reduce radiation dose
Improve contrast
Perform spectral analysis

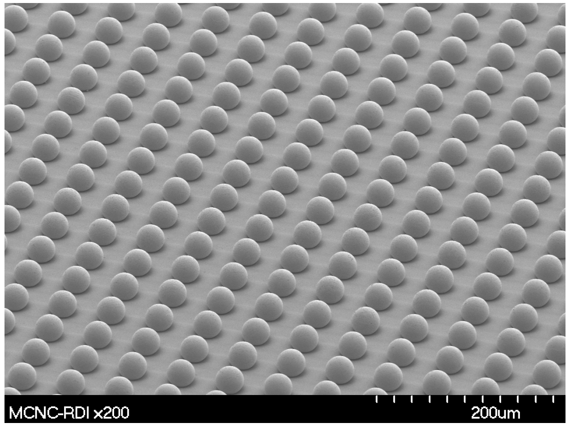

Courtesy: M Campbell, Medipix Collaboration, CERN

XPAD: X-ray Pixel chip with Adaptable Dynamics

Start of the hybrid pixel project

1991

1996

DELPHI
World
première

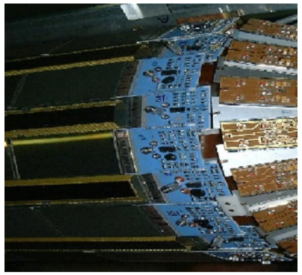

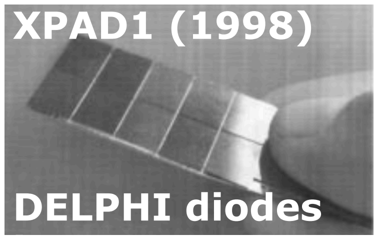

XPAD1: first hybrid pixel detector for X-ray detection

1998

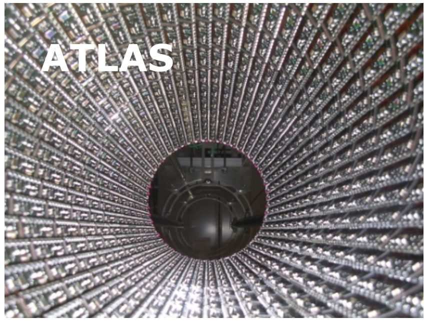

50 x 400 µm² pixels

2000

330 x 330 µm² pixels

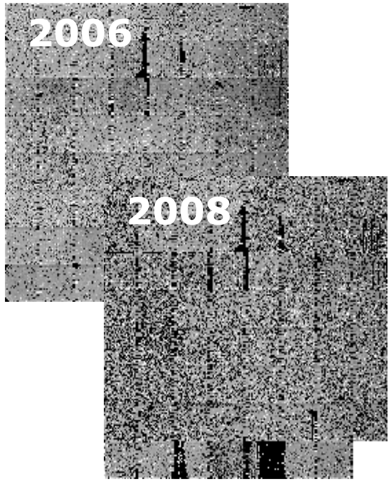

2006

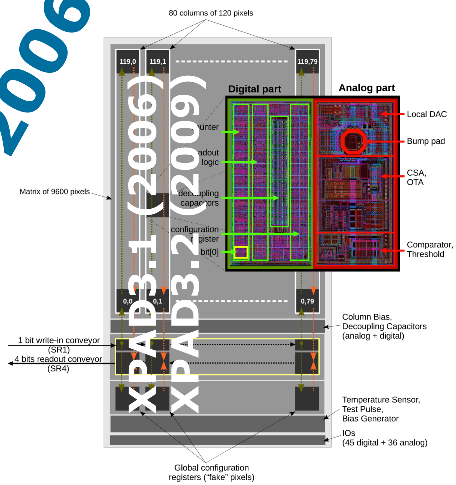

130 x 130 µm² pixels

Delpierre, JINST **9** (2014) C05059

XPAD3 Si and CdTe hybrid pixels for X-ray detetction

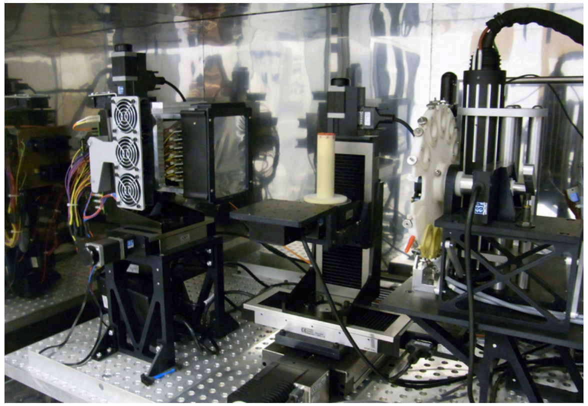

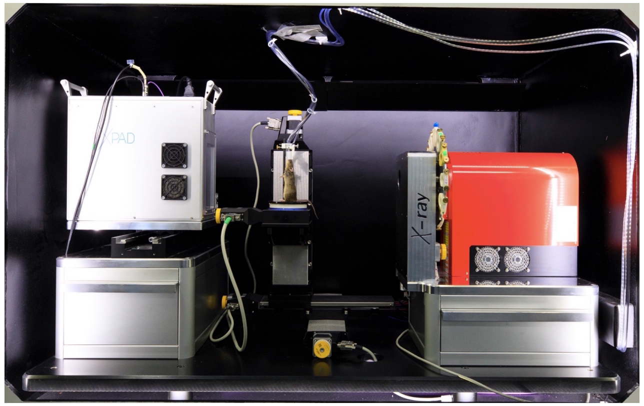

- XPIX: Development of the hybrid pixel detectors XPAD3.1 (2006) et XPAD3.2 (2009) with Si and CdTe sensors
  - > 0,5 Mpixels 130 x 130 µm^2
  - 240 images/s
  - 2011 • 5-35 keV (XPAD3.1/Si: D1-3)
  - 2013 • 5-60 keV (XPAD3.2/Si: D4-6)

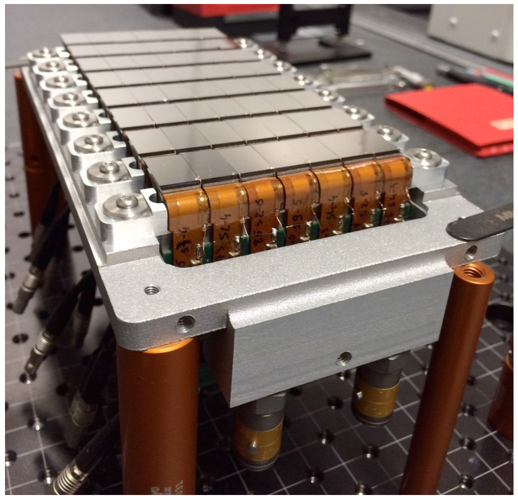

CHiPSpeCT

- 2015 • XPAD3.2/CdTe (D7)

XPAD3 pixel architecture

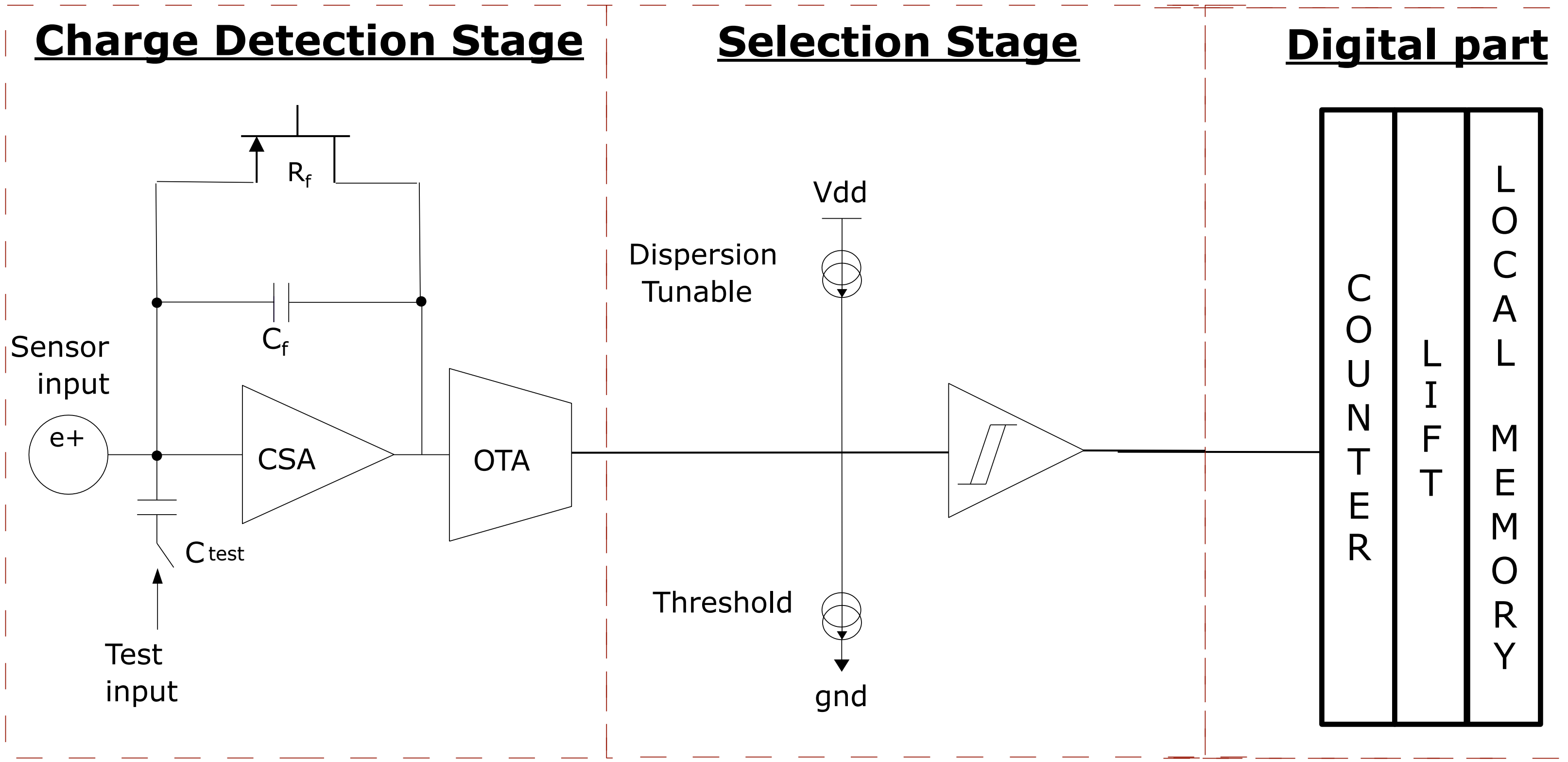

Gain : 89 nA/keV
Noise : 127 e- rms
Linearity : < 10% @ 35 keV

Power consumption : 40 µW/pixel
Threshold adjustment resolution : 57 e-
Minimum threshold: < 4 keV

XPAD3: Si and CdTe Hybrid Pixels for X-ray

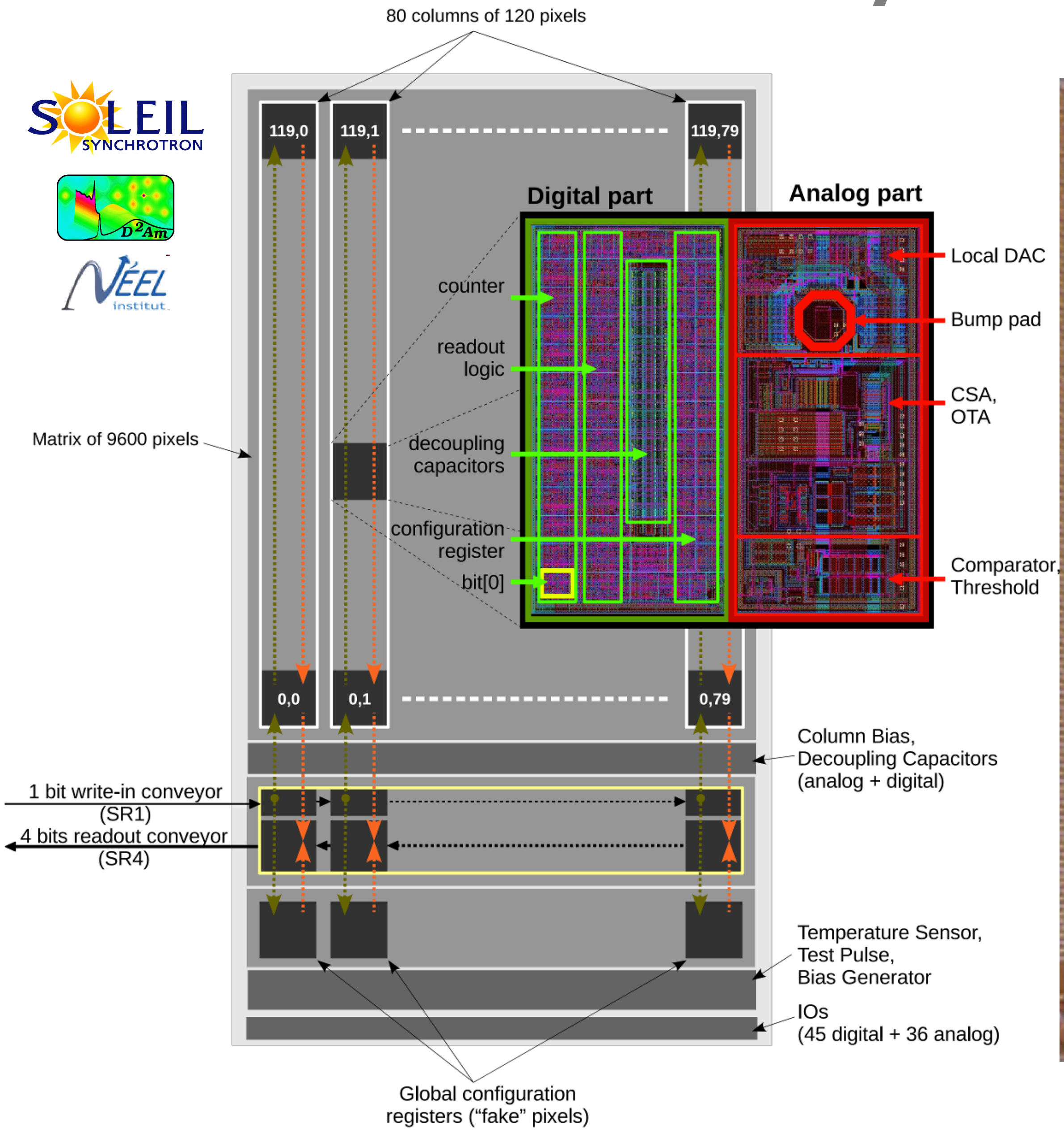

- 0.25 µm IBM CMOS technology
- (130 x 130) µm^2 pixels
- 80 x 120 = 9600 pixels
- 12 bit counter + overflow
- Count rate up to 10^6 ph/pixel/s
- < 1 ms readout time
- 5-35 keV adjustable thresholds

XPAD3 Camera : 500,000 pixels of 130 µm

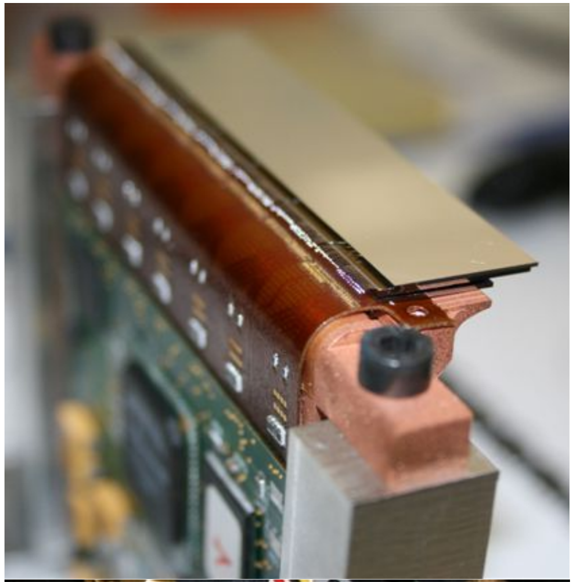

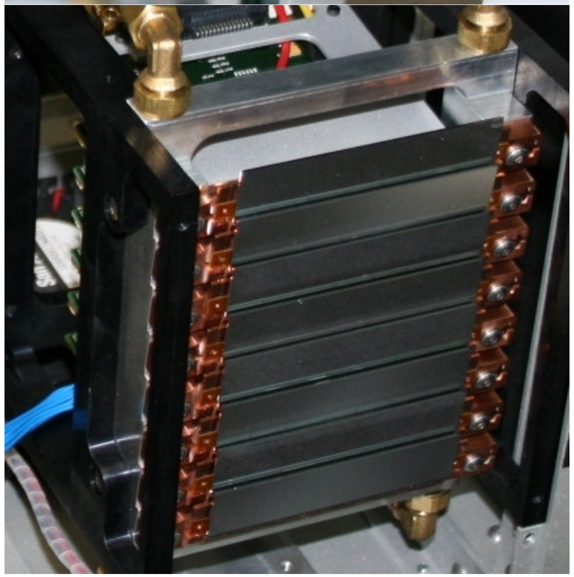

5 keV

SOLEIL SYNCHROTRON

14 keV

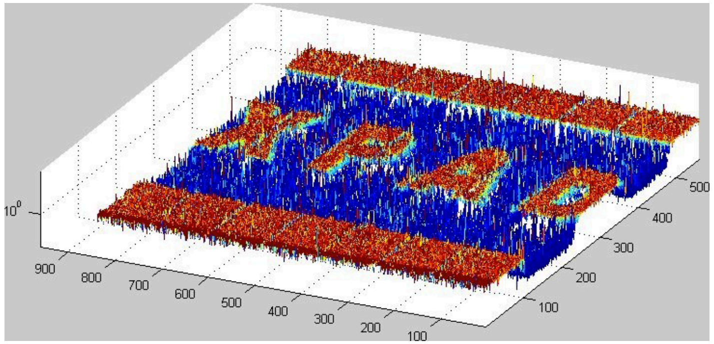

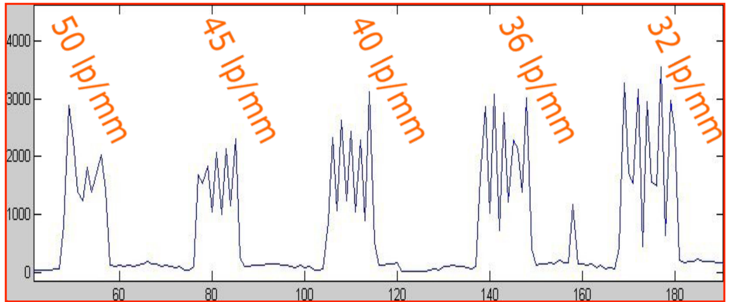

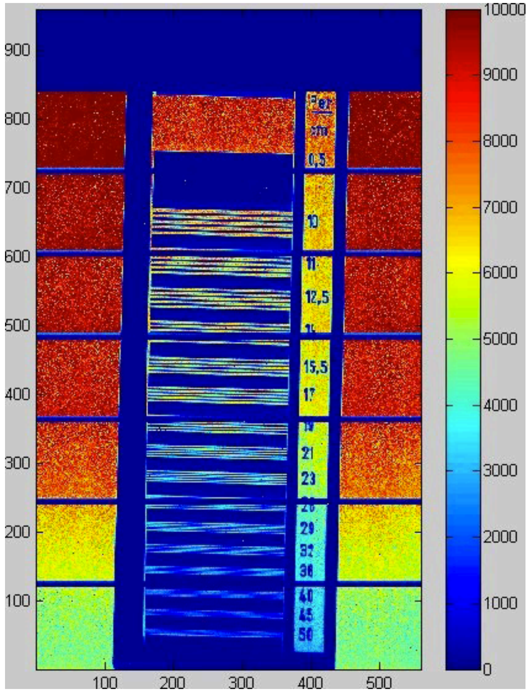

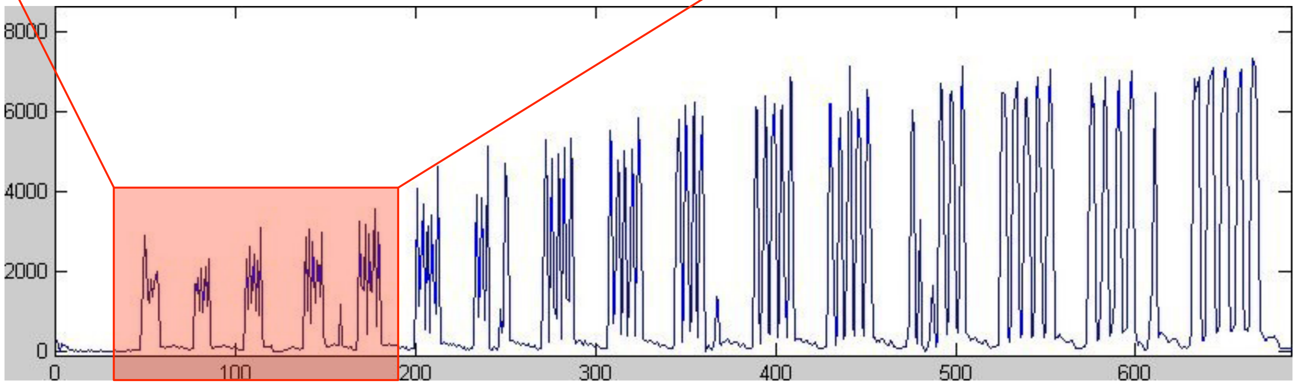

Aix*Marseille université CNRS IN2P3 Les deux infinis CPPM

First longitudinal study of liver tumour development in mice

In vivo imaging protocole

- Standard absorption imaging
- Anaesthesia: 3 % Isoflurane
- Source: 50 kV/500 µA/0.6 mm Al
- Scan type: continuous
- Exposition duration: 575 ms + 50 ms DT
- Projections: 720 (0.5°)
- Delivered dose: 177 mGy/acquisition

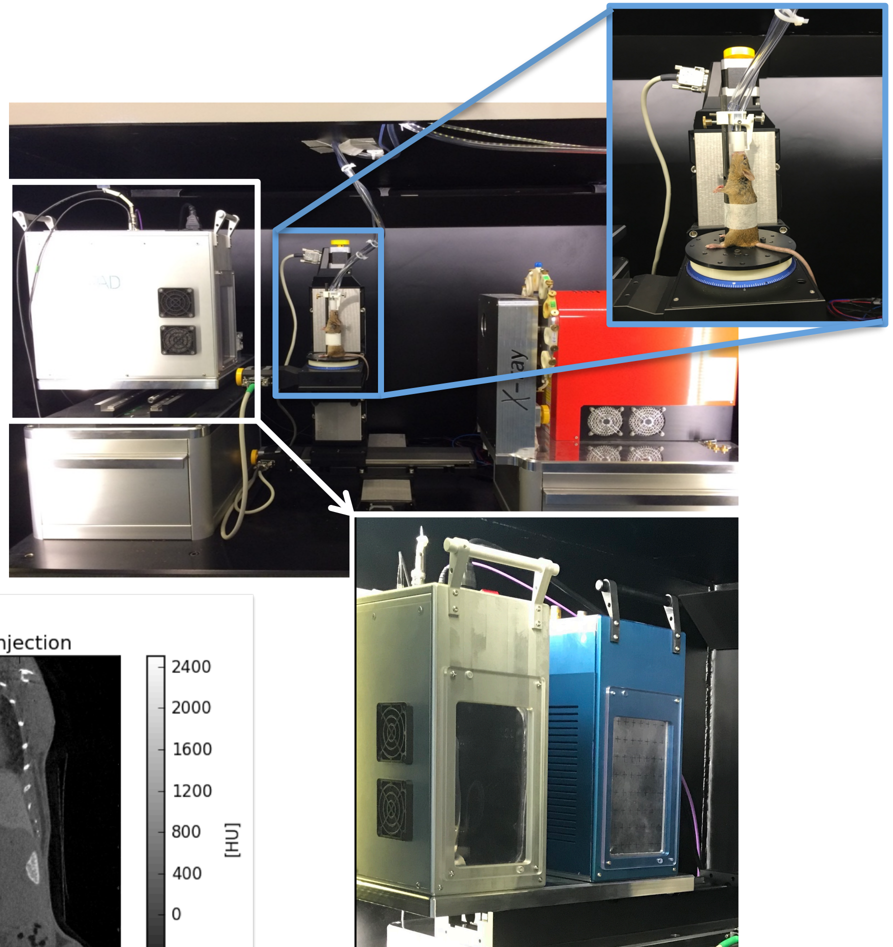

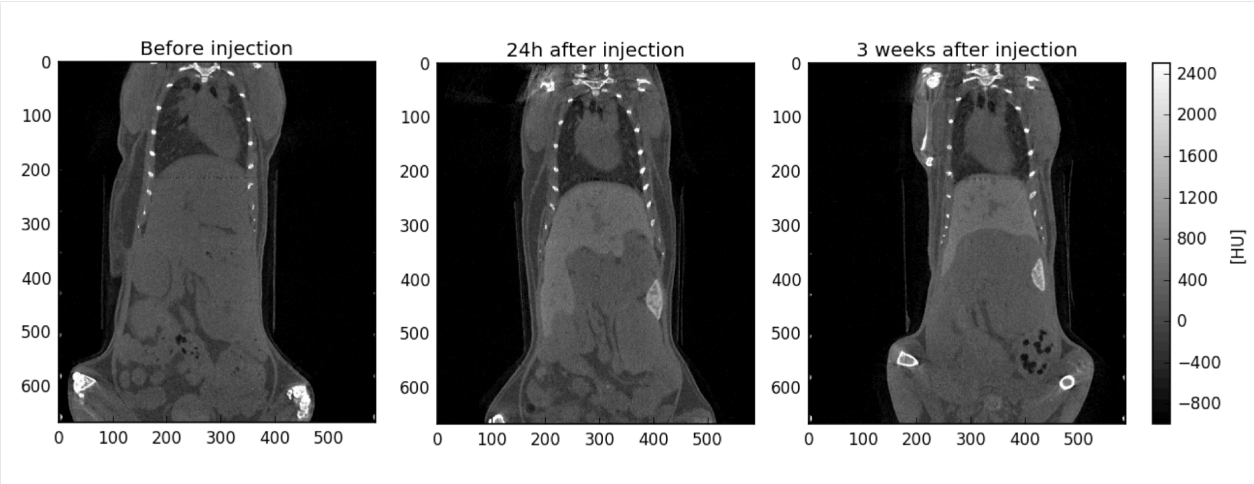

Coronal slices of a the same mouse labelled with 100 µL/30g of Exitron nano 12000

First longitudinal study of liver tumour development in mice

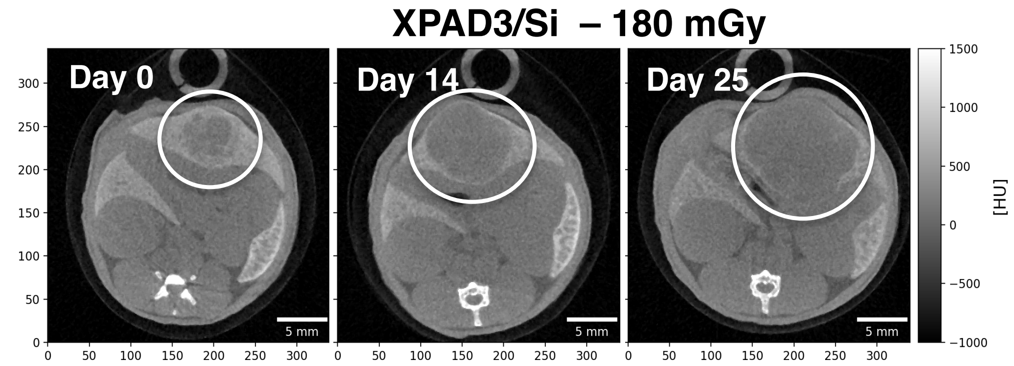

Follow up of a mouse with an hepatocellular carcinoma for one month

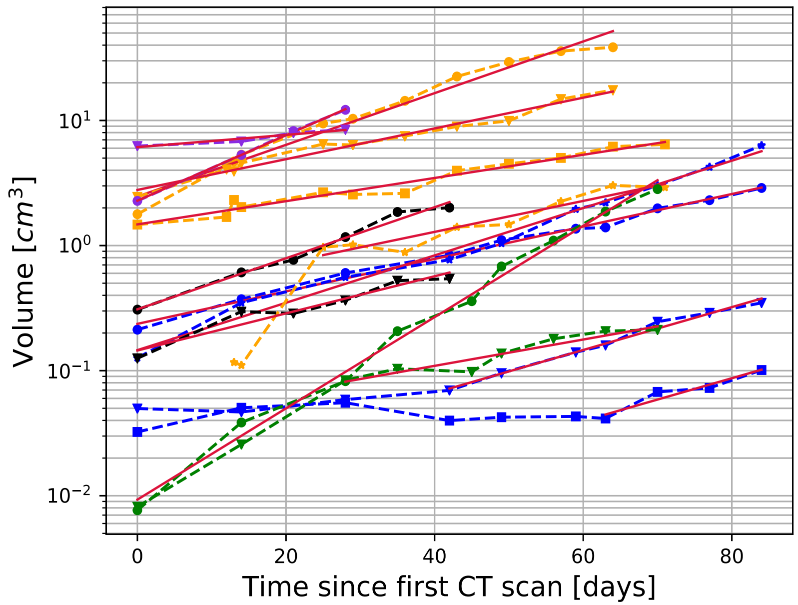

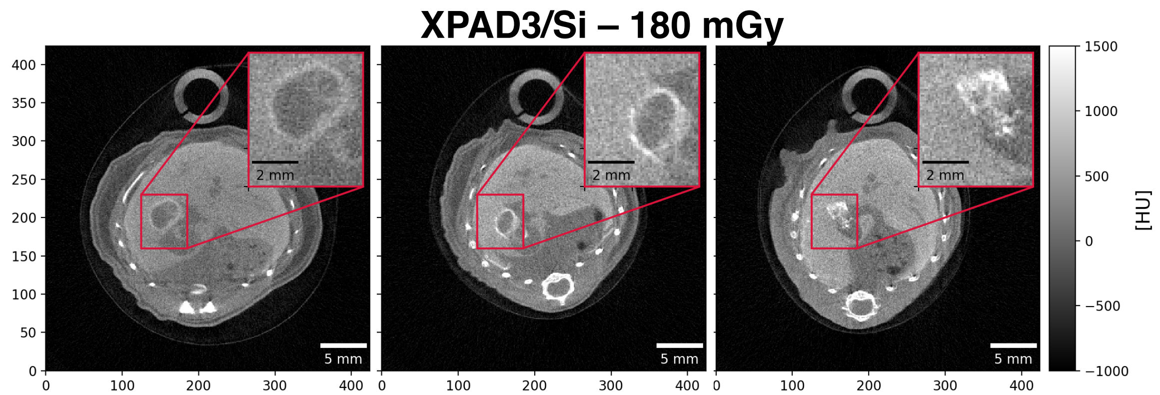

Monitoring of the treatment response to an hepato-specific therapy (Mek + Bcl-XL inhibition*) for 40 days

*Y. Fan et *al.*, Hepatology 66 (2017)

Workshop on
Medical Applications of Spectroscopic X-ray Detectors
CERN, 20-23 April 2015

Name	Matrix	side (µm)	Energy thresholds	Peaking time (ns)	Maximum count rates (Mcps/pixel)	Maximum count rates (Mcps/mm²)	Electronics Noise or energy resolution	Power per channel (µW)	CMOS node
Medipix3 (FPM-SPM)[1]	256x256	55	2	120	2.5	826.5	1.37keV FWHM @ 10KeV	7.5	0.13µm
Medipix3 (FPM-CSM)[2]	256x256	55	1+1	120	5.0E-01	163.5	2.03keV FWHM @10KeV	9.3	0.13µm
Timepix3 (CERN)[3]	256x256	55	10bits	30	1.6E-03	0.53	4.07kev FWHM at 59.5keV	15.2	0.13µm
Pixirad Pixie II[4]	512x476	55.6	2	300	5.0E-01	161.5	1.45keV FWHM @ 20keV	12.5	0.18µm
Samsung PC[5]	128x128	60	3	NS	NS	NS	68 e- r.m.s.	4.6	0.13µm
Pixirad Pixie III[6]	512x402	62	2	125	1.0	260.1	6.6% FWHM @ 60keV	34	0.16µm
Eiger[7]	256x256	75	1	30	4.2	711.1	121e- r.m.s. (low noise settings)	8.8	0.25µm
PXD23K (AGH)[8]	128x184	75	2	48	8.5	1519.5	89e- r.m.s.	25	0.13µm
X-Counter PC (PDT25-DE)[9]	256x256	100	2	NS	1.2	120	8.3keV FWHM @20keV 10keV FWHM @60keV	NS	NS
PXD18K (AGH)[8]	96x192	100	2	30	5.8	580	168e- r.m.s.	23	0.18µm
FPDR90 (AGH)[8]	40x32	100	2	28	8.5	854.7	106e- r.m.s.	42	90nm
AGH_Fermilab[10]	18x24	100	2	48	NS	NS	84e⁻ (Single pixel), 168e⁻ (Charge summing)	34	40nm
Medipix3 (SM-SPM)[11]	128x128	110	8	120	4.5	375.7	1.43keV FWHM @ 10keV	30	0.13µm
Medipix3 (SM-CSM)[12]	128x128	110	4+4	120	3.4E-01	28.1	2.2keV FWHM @10keV	37.2	0.13µm
XPAD3[13]	80x120	130	2	150	2.0	118.3	127e- r.m.s.	40	0.25µm
Pilatus 2[14]	60x97	172	1	110	6.0	202.8	1keV FWHM @ 8keV	20.2	0.25µm
Pilatus 3[15]	60x97	172	1	110	15.0	507.0	1keV FWHM @ 8keV	20.2	0.25µm
Telesystems [16]	40x40	200	4	300-500	8.0E-01	20	5.36keV FWHM @ 122keV	94.4	0.25µm
Dosepix (CERN)[17]	16x16	220	16	287	1.6	33.9	150 e- r.m.s.	14.6	0.13µm
Siemens PC[18]	64x64	225	2	20	40.0	790.1	NS	NS	NS
Hexitec[19]	80x80	250	14bits	2000	1.0E-03	0.016	800eV FWHM @ 60keV, 1.1keV @ 141keV	220	0.35µm
Philips Chromaix [20]	4x16	300	4	20	38.0	422.2	4.7keV @60keV (1 channel)	3000	0.18µm
Ajat-0.35 (PC)[21]	32x64	350	1	1000	2.2	18.0	4keV FWHM @122keV	390.6	0.35µm
Ajat-0.35 (ADC)[22]	32x64	350	64	1000	4.9E-05	4.0E-04	4keV FWHM @122keV	390.6	0.35µm
CIX 0.2 (Bonn)[23]	8x8	353.6	1	NS	12.0	96	330e- r.m.s. (counting channel)	3200	0.35µm
KTH_Lin_SPD [24]	160 ch.	447.2	8	10-20-40	272.0	1360	1.09keV @ 15keV (measured at 40kcps)	80000	0.18µm
DxRay-Interon[25]	16x16	500	4	10	13.3	53	7keV FWHM @60keV, Min TH20keV	NS	NS
Ajat-0.5[26]	44x22	500	2	1000-2000	NS	NS	4.7keV @122keV (1 channel)	413.2	0.35µm
Hamamatsu[27]	64 ch.	632.5	5	NS	5.5	13.75	12keV FWHM @ 120keV	NS	NS
IDEAS[28]	64 ch.	894.4	6	50	4.0	5	7keV FWHM @60keV	4200	0.35µm
GE-DxRay [29]	128 ch.	1000	2	30	11.6	11.6	4.75% at 122keV, CZT, 5pF Cin (1 Channel noise= 4.8keV FWHM)	2100	0.25µm
BNL [30]	64 ch.	1241.0	5	40-80-160-320	4.0	5.5	5.5keV at 40ns peaking time/2.15keV at 320ns peaking time	4700	0.25µm

Courtesy: R. Ballabriga, Medipix Collaboration, CERN

Medipix3/Si RX images

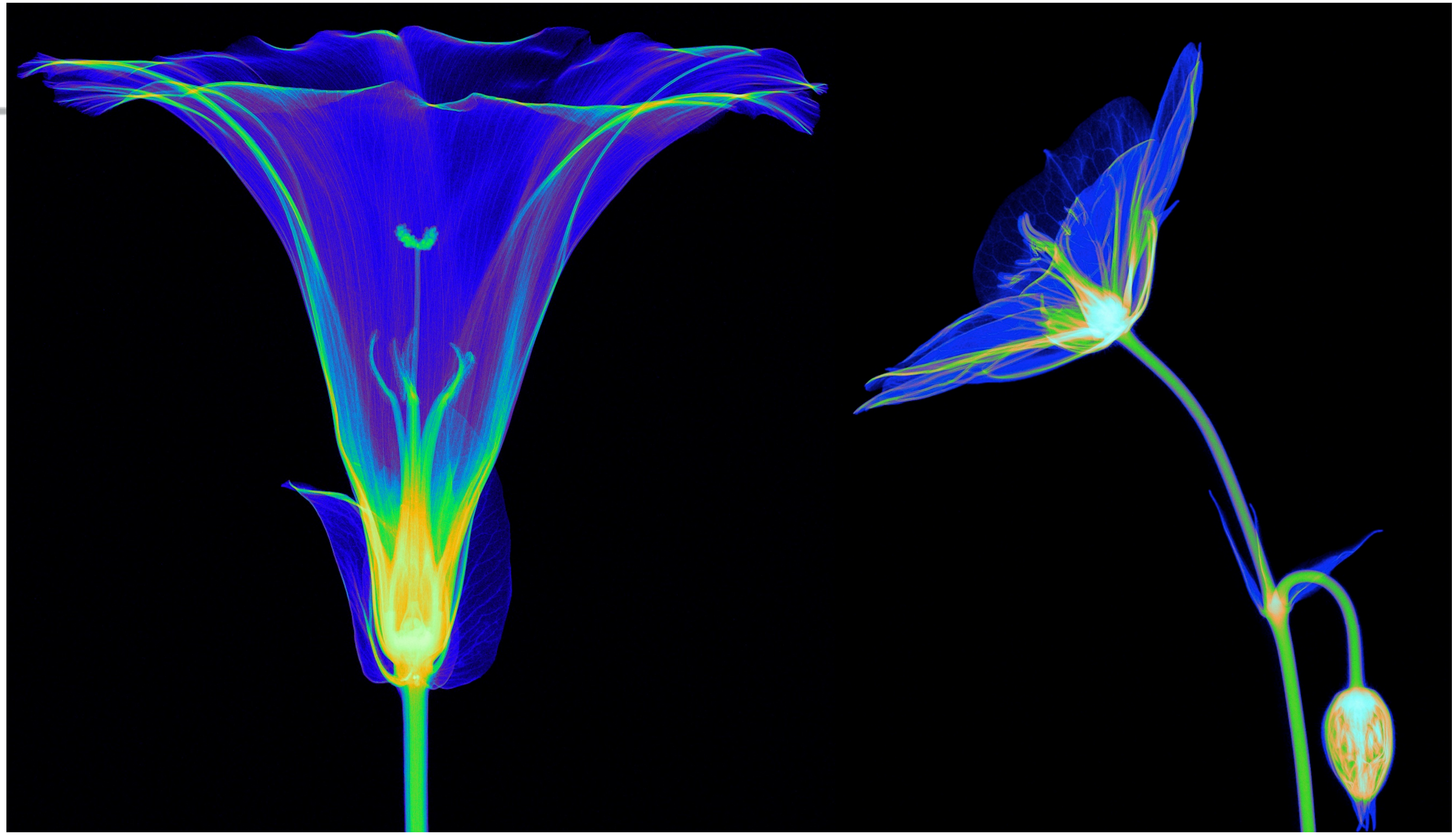

Courtesy: S. Procz, Medipix Collaboration, CERN

- Medipix3/Si 55µm SPM HGM 24-Bit, 8 x 8 tiles
- 20kV / 100µA, Mag. 2x
- Object width ~45 mm

Hybrid pixels: many spin-offs

2003
DxRay
www.dxray.com

2006
DECTRIS®
www.dectris.com

2010
imXPAD
www.imxpad.com

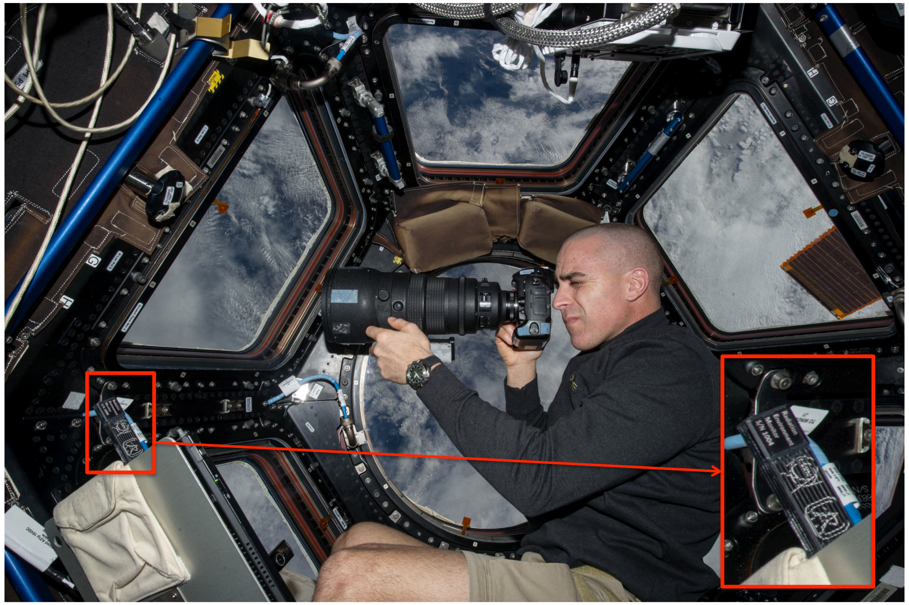

Courtesy: NASA, photo ref. no. iss036e006175

2006
XRAY IMATEK
Pixelated X-Ray Detectors
www.xray-imatek.com

2011
PiXirad
Chromatic Photon Counting
pixirad.pi.infn.it

2011
asa AMSTERDAM SCIENTIFIC INSTRUMENTS
www.amscins.com

2012
ADVACAM
IMAGING THE UNSEEN
www.advacam.com

2011
XIE X-RAY IMAGING EUROPE
www.xi-europe.com

2003
kromek
detect image identify
www.kromek.com

2007
mars
Medipix All Resolution System
www.marsbioimaging.com

Sensors for direct X-ray detection

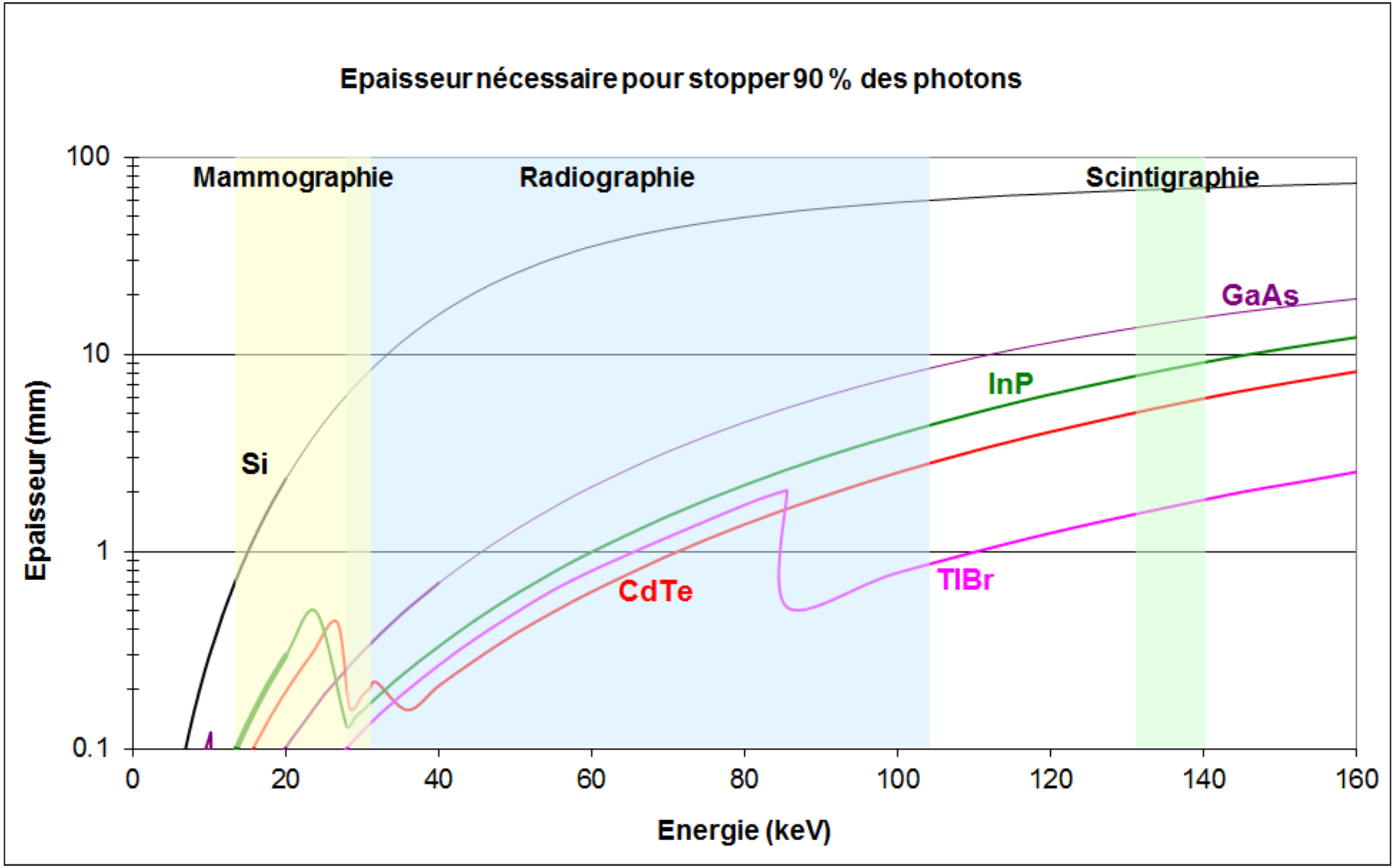

Courtesy: E. Gros d'Aillon, CEA-LETI

What are the differences ?

	Z	ρ (g/cm³)	E_{gap} (eV)	E_{e-h} (eV)	μ_e (cm²/V/s)	τ_e (s)	μ_h (cm²/V/s)	τ_h (s)	$\mu_e\tau_e$ (cm²/V)	$\mu_h\tau_h$ (cm²/V)
Diamond	6	3.52	5.5	13.0	4500		3800			
Si	14	2.32	1.12	3.62	1400	1×10^{-3}	480	2×10^{-3}	1.4	0.96
Ge	32	5.33	0.67	2.95	3900	1×10^{-3}	1900	1×10^{-3}	3.9	1.9
GaAs	32	5.32	1.43	4.30	8000	1×10^{-8}	400	1×10^{-7}	8×10^{-5}	4×10^{-5}
$Cd_{0.9}Zn_{0.1}Te$	49.1	5.78	1.57	4.64	1000	3×10^{-6}	50	1×10^{-6}	3×10^{-3}	5×10^{-5}
CdTe	50	5.85	1.44	4.43	1100	3×10^{-6}	100	2×10^{-6}	3.3×10^{-3}	2×10^{-4}

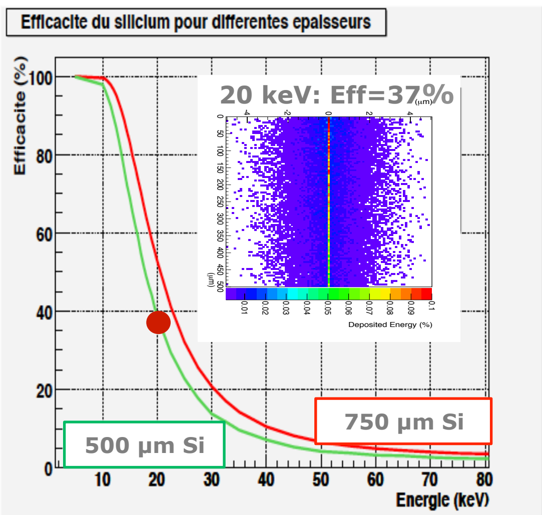

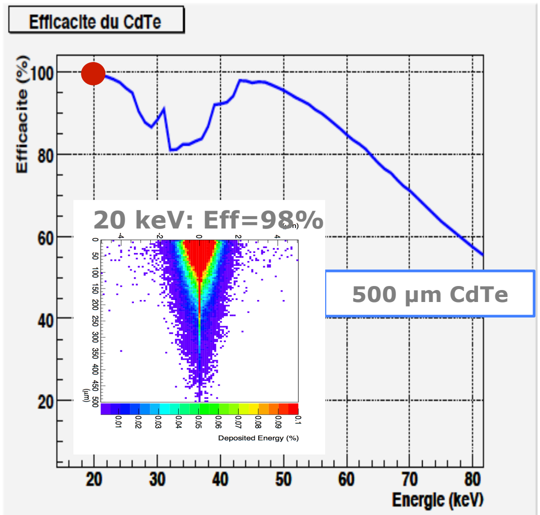

K-edge Cd : 26.7 keV

K-edge Te : 31.8 keV

K-alpha Cd : 23.1 keV

K-alpha Te : 28.4 keV

Medipix3 Image (GaAs 55 µm/500 µm)

A tiled X-ray image of a mouse skull

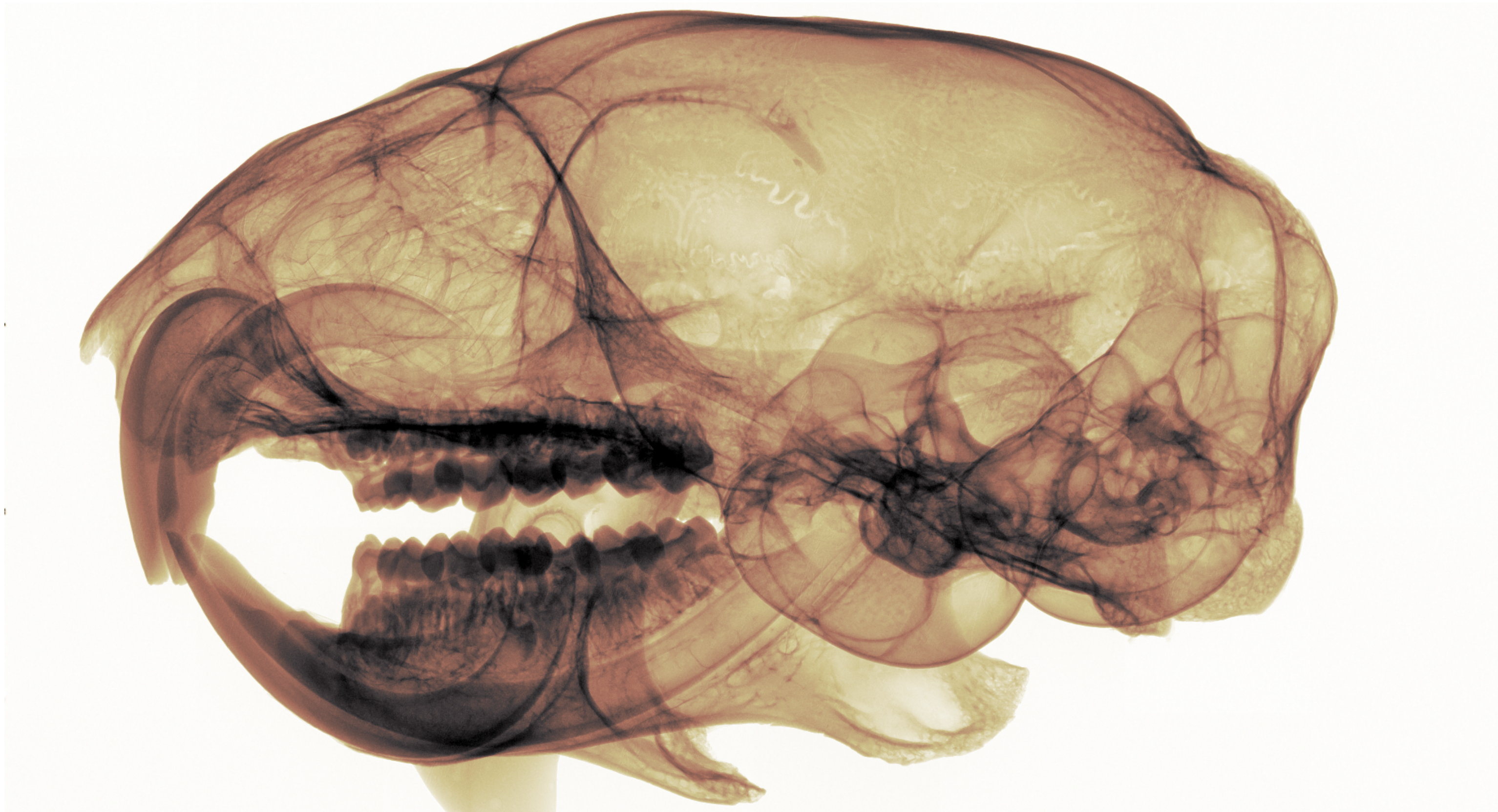

Courtesy: S. Procz, Medipix Collaboration, CERN

ChiPSpeCT & CALIPSO: XPAD3-2/CdTe camera

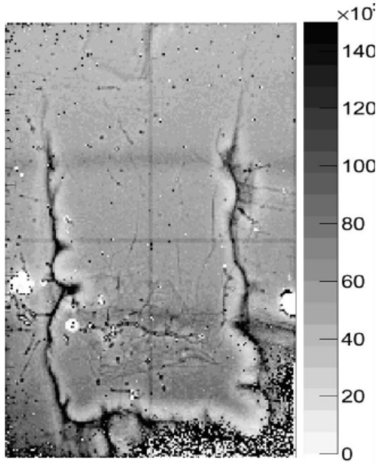

XPAD3 « Quad »

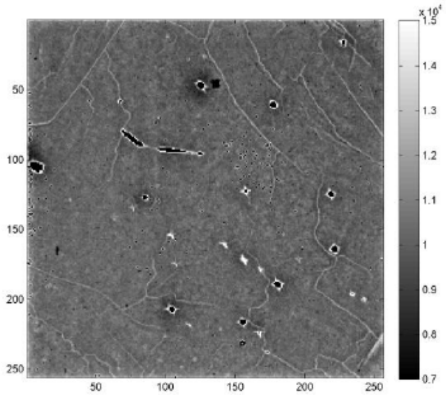

Medipix2 « Quad »

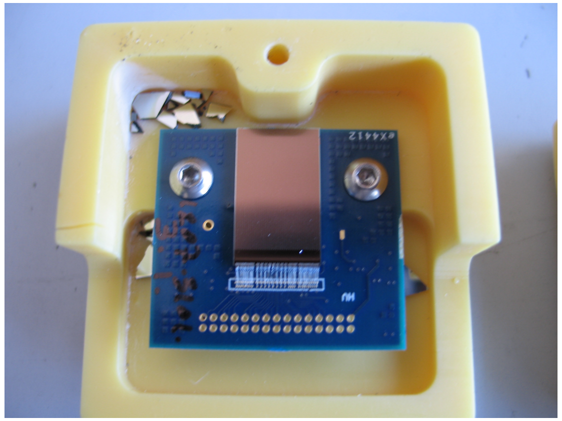

June 7 2013

- HighZpad (FP7 ELISA)
  - « Survey » of state-of-the-art high-Z sensors and of hybridization methods to get large surface detectors
  - 3 pixel circuits considered (Medipix2, Pilatus, XPAD3)
  - One « hybridizer » : XIE, indium bumps
  - CdTe sensors for « Quads » (Acrorad)
  - For all the considered circuits, there were hybridization problems or impairing of sensors generating spots and high leakage currents.

Construction of the CHiPSpeCT camera

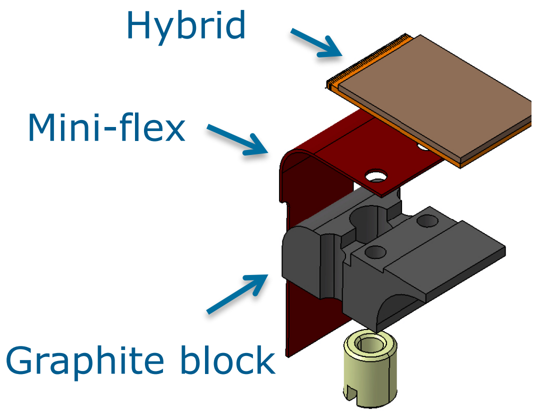

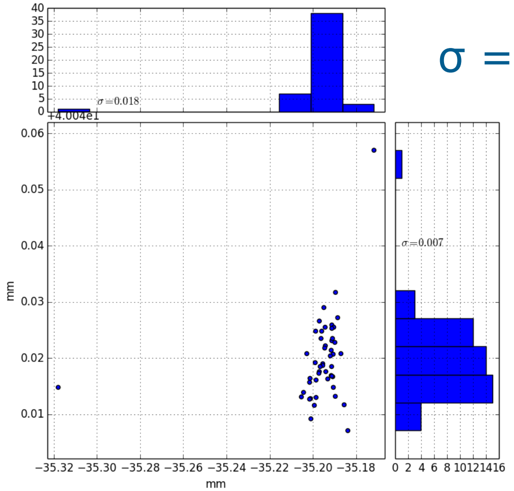

σ = 0.018 mm

σ = 0.007 mm

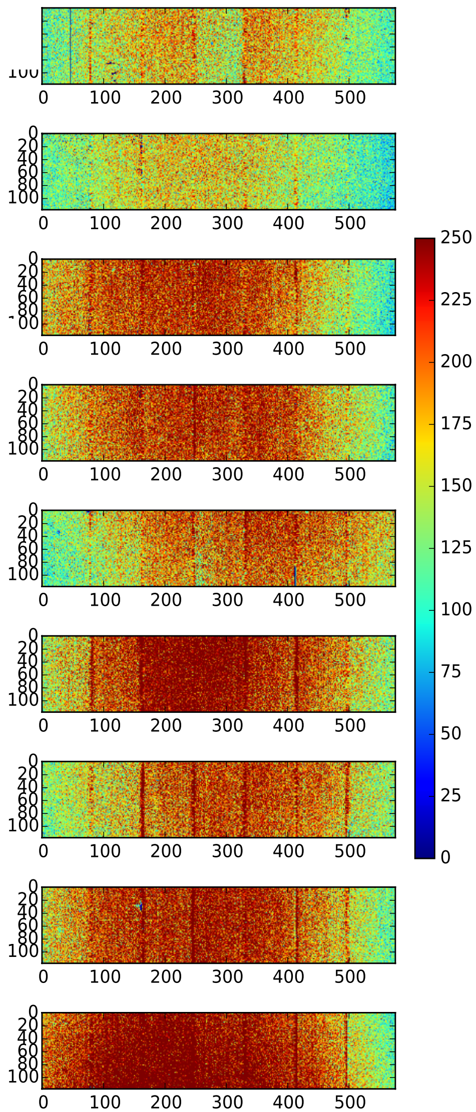

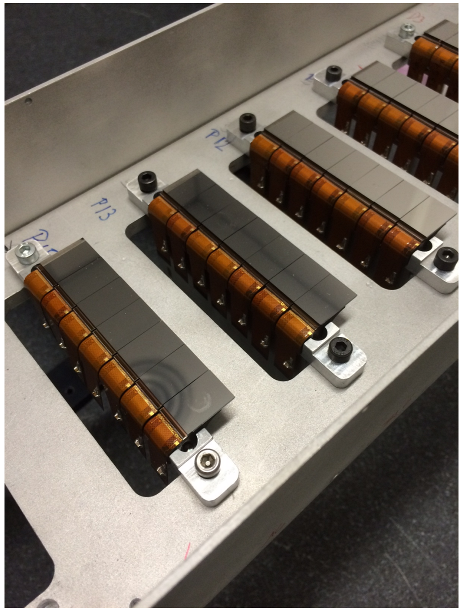

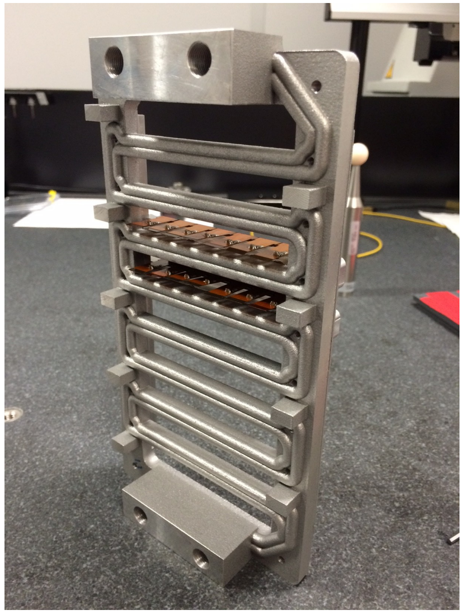

First irradiations on the D2AM ESRF beam line at at 25.5 keV

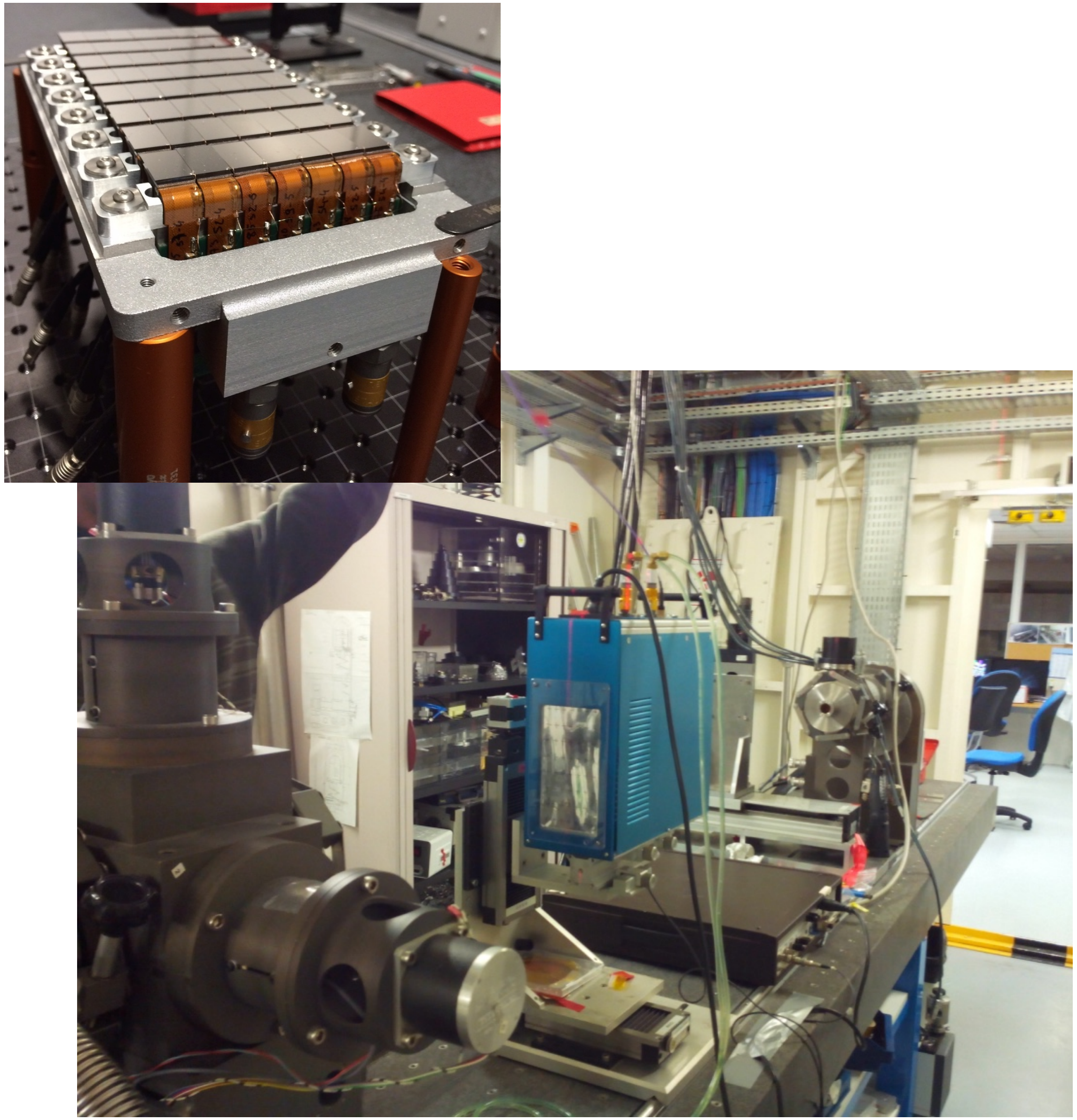

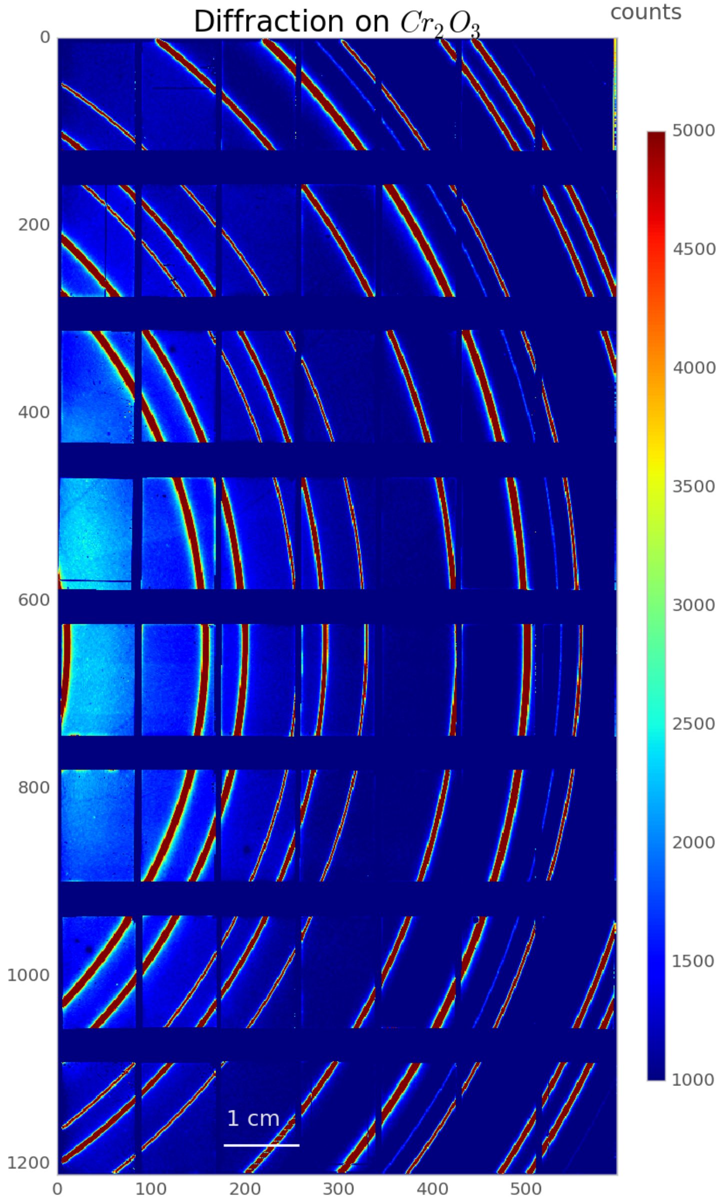

CdTe versus Si for standard absorption CT

- Dose reduction x 10 for E > 30 keV

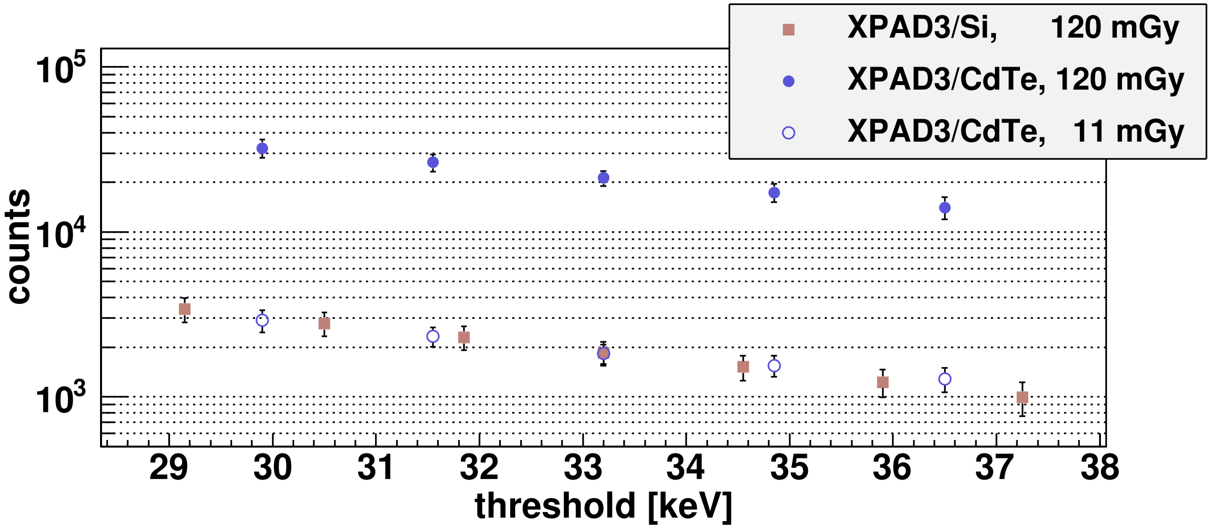

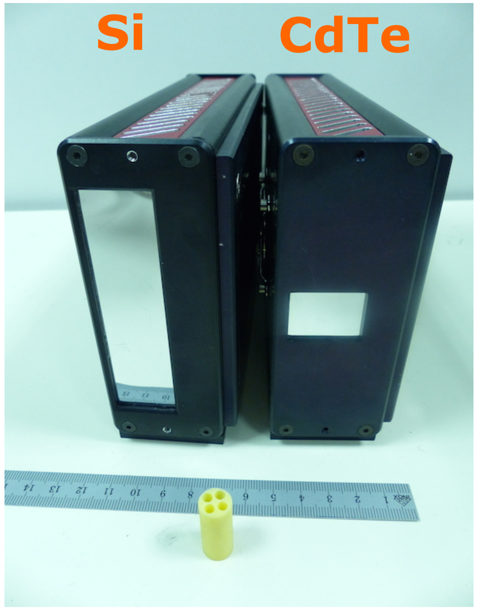

120 mGy → 11 mGy

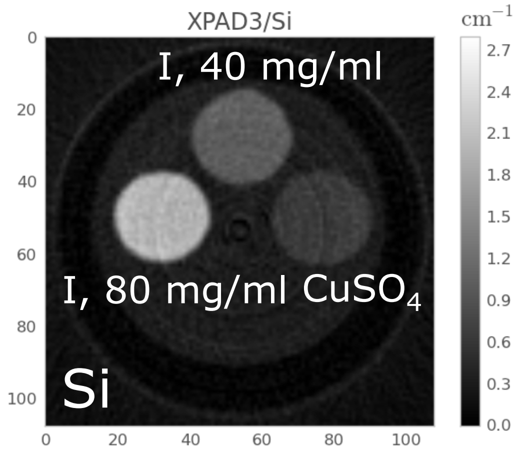

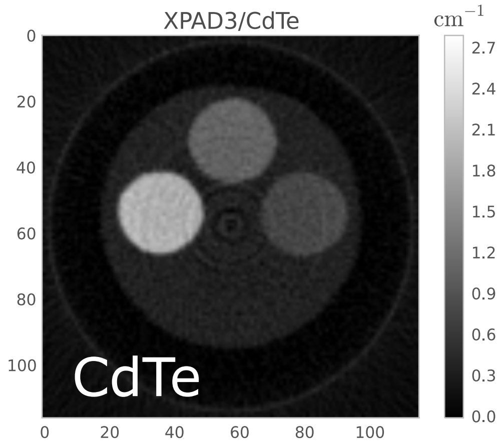

For equivalent stats

F. Cassol et al. Phy.s Med. Biol. 60 (2015)

Spectral CT: from black & white to colour

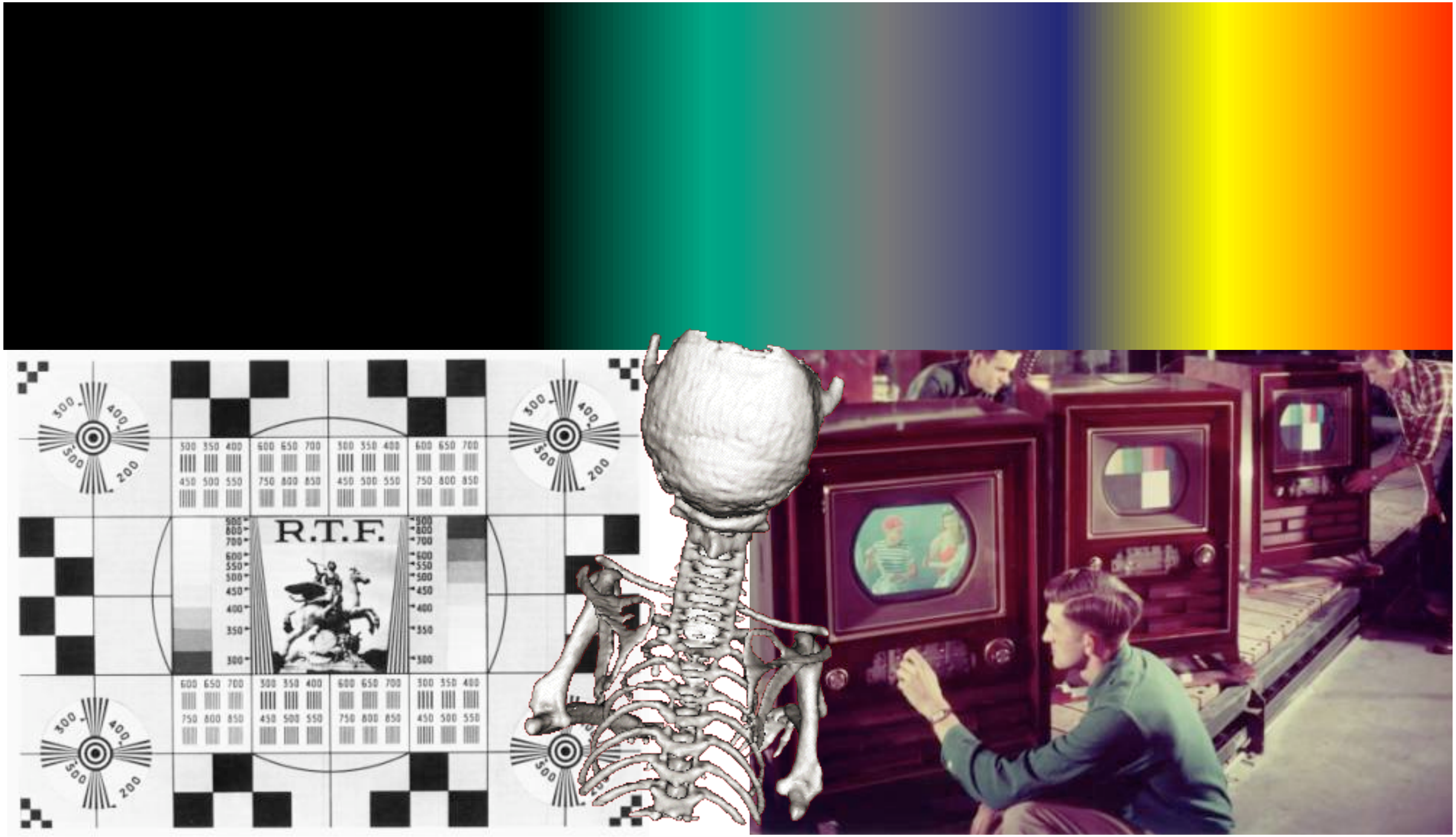

Ecole d'été France Excellence, Marseille, 1-11 Jul 2019

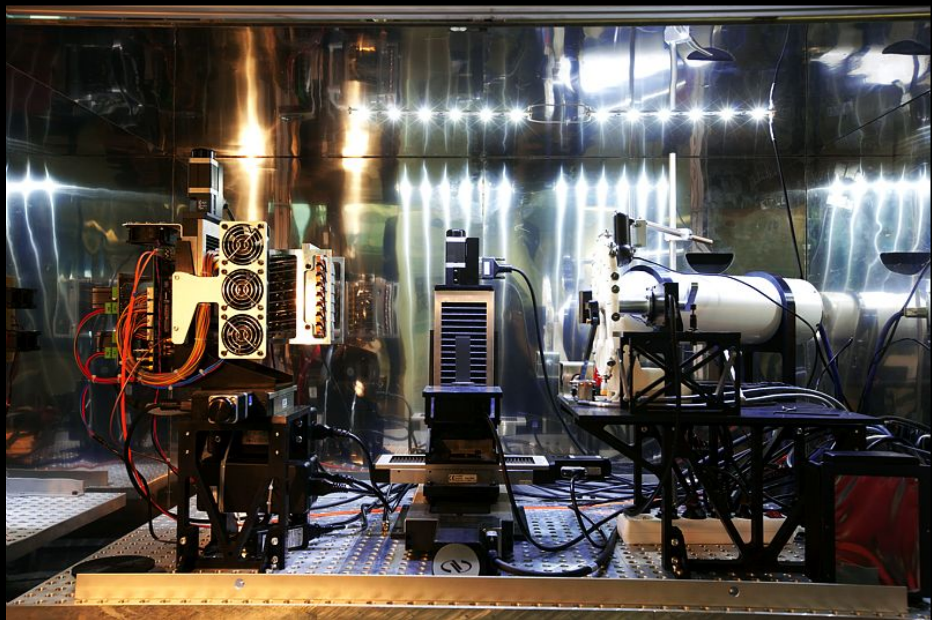

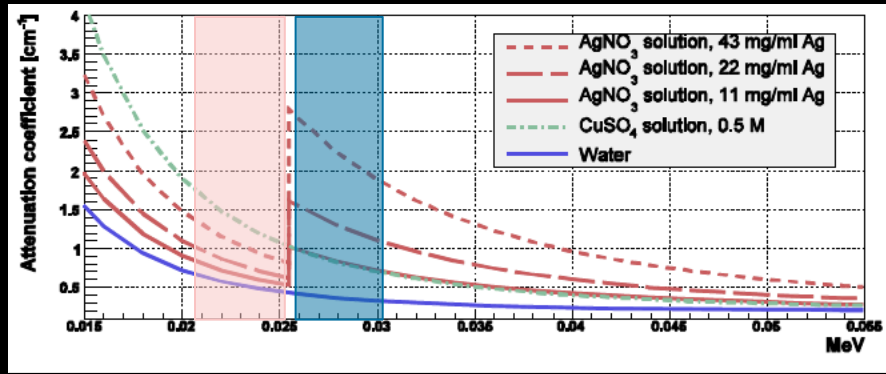

Attenuation coefficient [cm^{-1}]
MeV
$AgNO_3$ solution, 43 mg/ml Ag
$AgNO_3$ solution, 22 mg/ml Ag
$AgNO_3$ solution, 11 mg/ml Ag
$CuSO_4$ solution, 0.5 M
Water

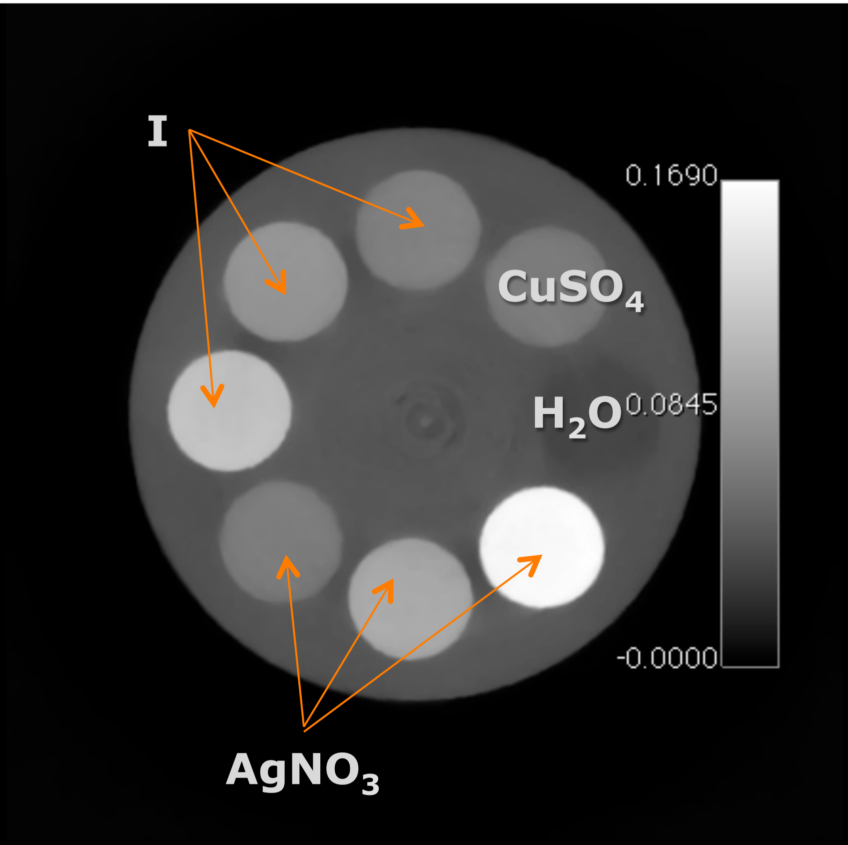

I
$CuSO_4$
H_2O
$AgNO_3$
0.1690
0.0845
-0.0000

X-ray spectral CT using XPAD3

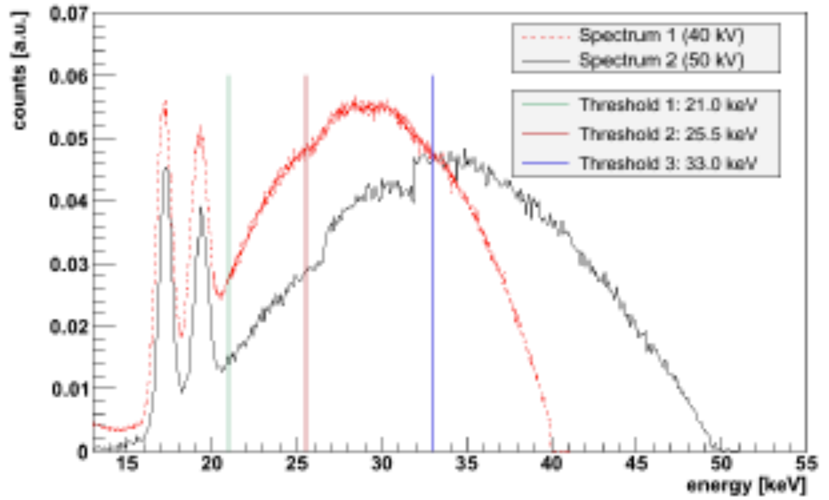

Silver	Iodine
$E_{1Ag} = 21$ keV	$E_{1I} = 25.5$ keV
$E_{2Ag} = 25.5$ keV	$E_{2I} = 33$ keV
$E_{3Ag} = 33$ keV	$E_{3I} = 40/50$ keV

Standard CT

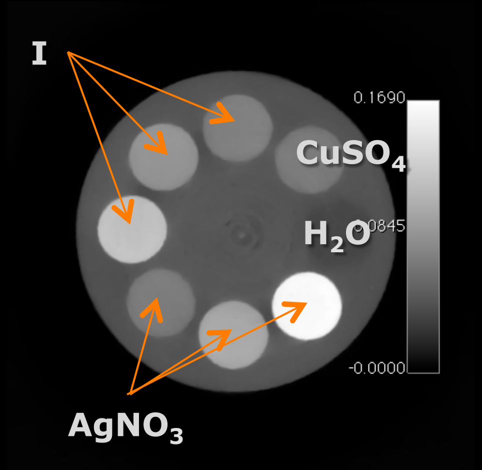

Iodine and Silver K-edge imaging

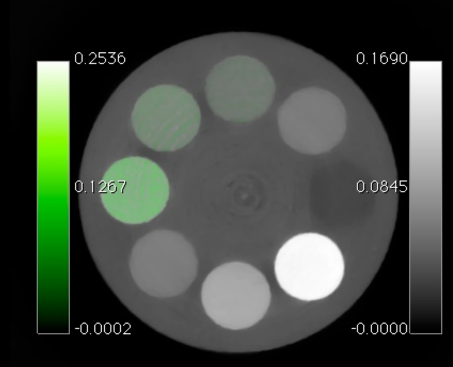

$(E_{2I} - E_{3I}) - (E_{1I} - E_{2I})$

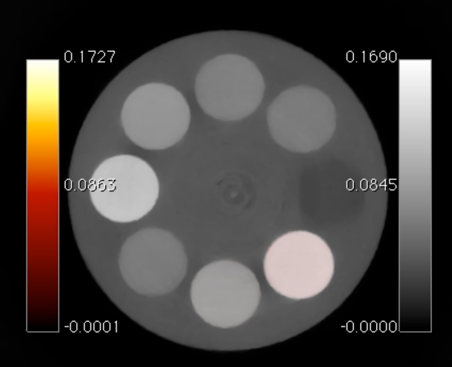

$(E_{2Ag} - E_{3Ag}) - (E_{1Ag} - E_{2Ag})$

Cassol *et al.*, IEEE Trans. Nucl. Sci. 60 (2013) 103

X-ray spectral CT using XPAD3

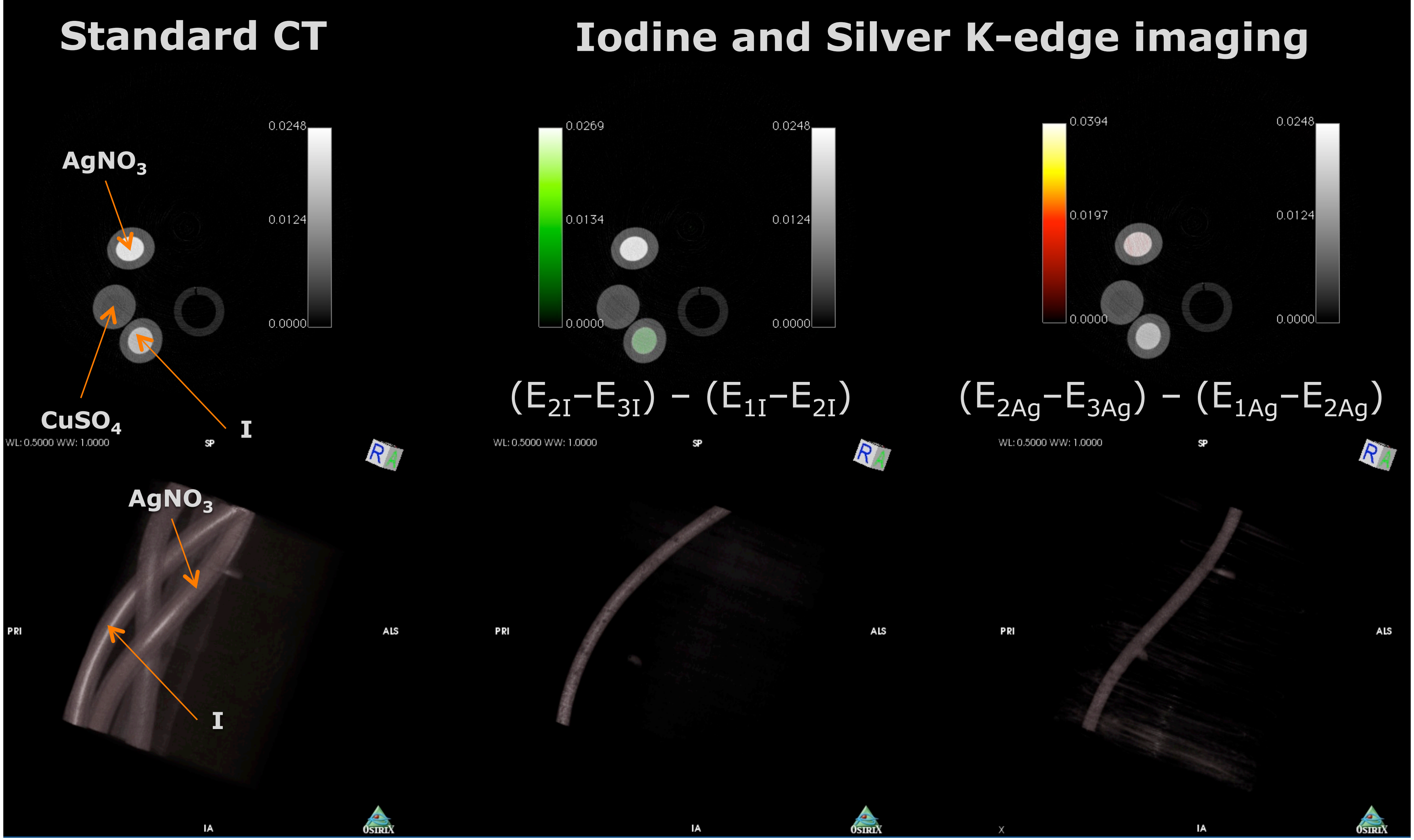

Cassol *et al.*, IEEE Trans. Nucl. Sci. 60 (2013) 103

Spectral CT: a novel intrinsically anatomo-functional modality

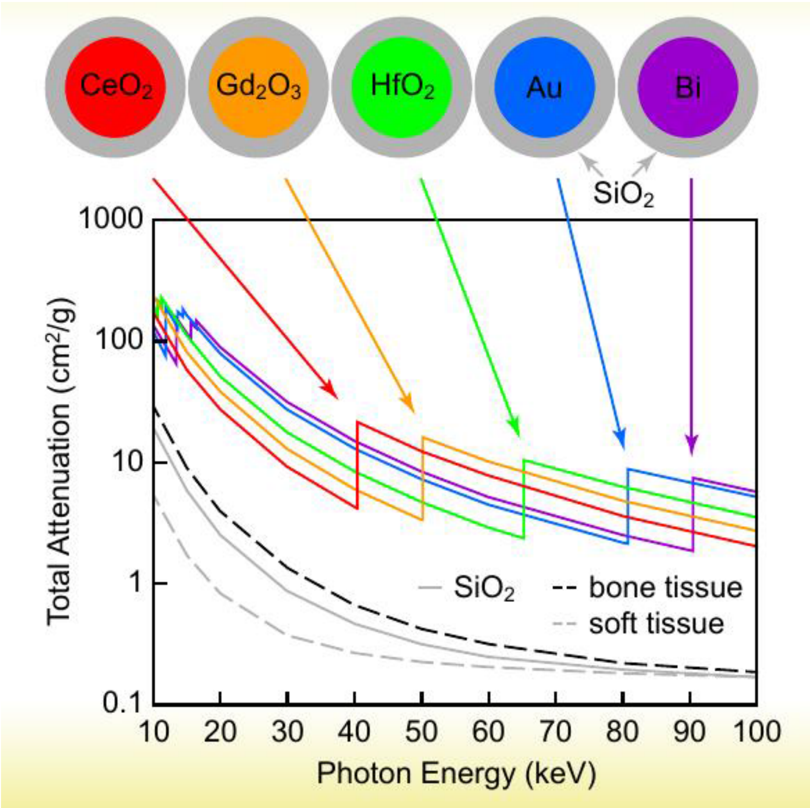

L.E. Cole et al. Nanomedicine 10 (2015) 321

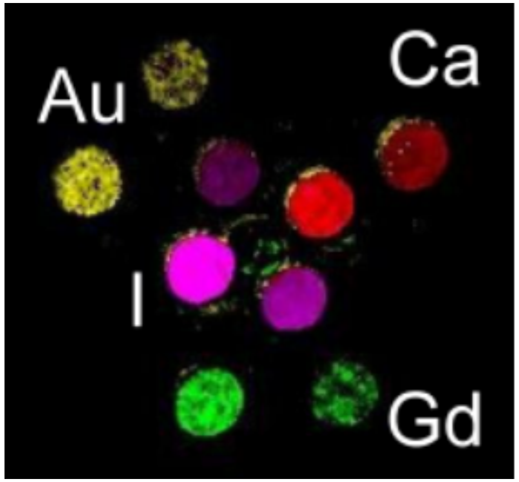

MARS image using human energy range (CdTe-MedipixRX)

Courtesy: A Buttler, Medipix Collaboration, CERN

K-edge imaging of iodine using composite pixels with XPAD3

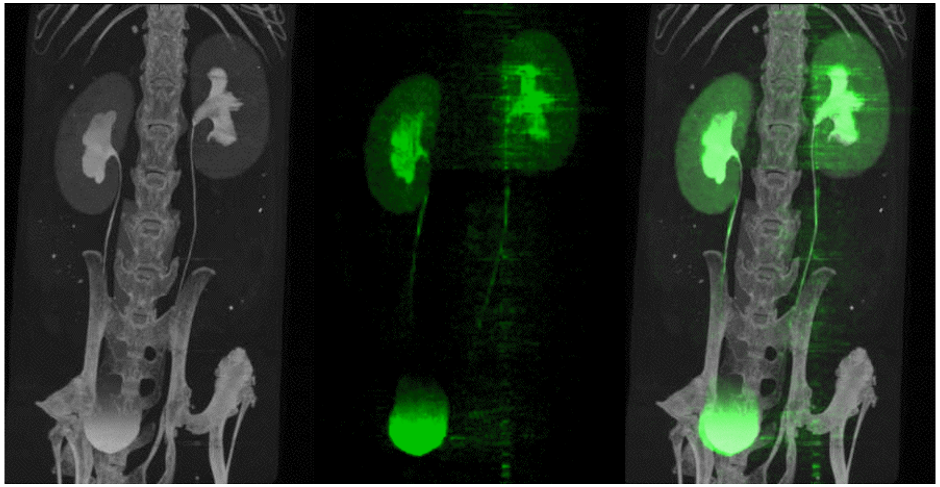

In vivo barium K-edge imaging

Preliminary phantom tests

→ Identification of concentrations > 25 mg/ml

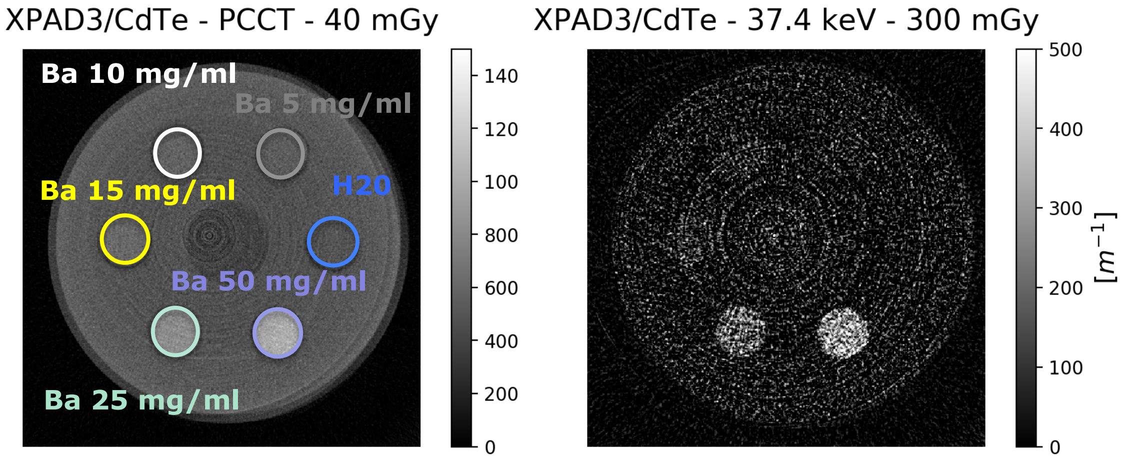

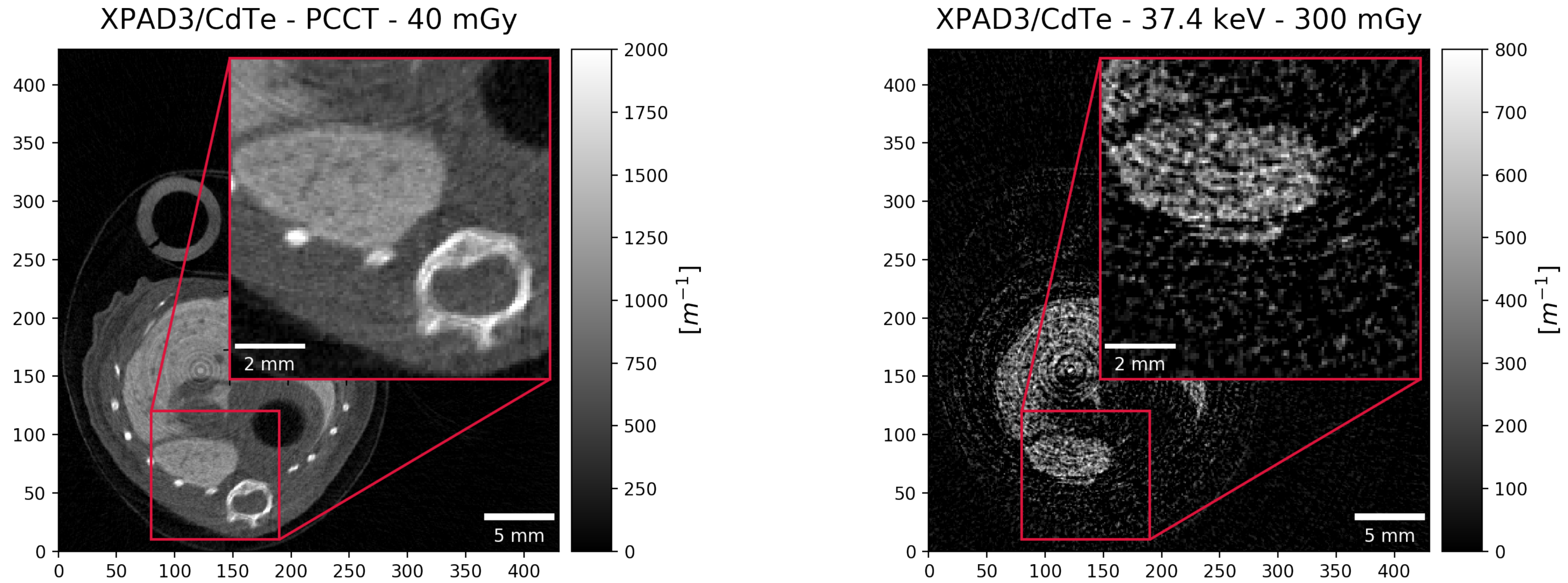

Positron Emission tomography (PET)

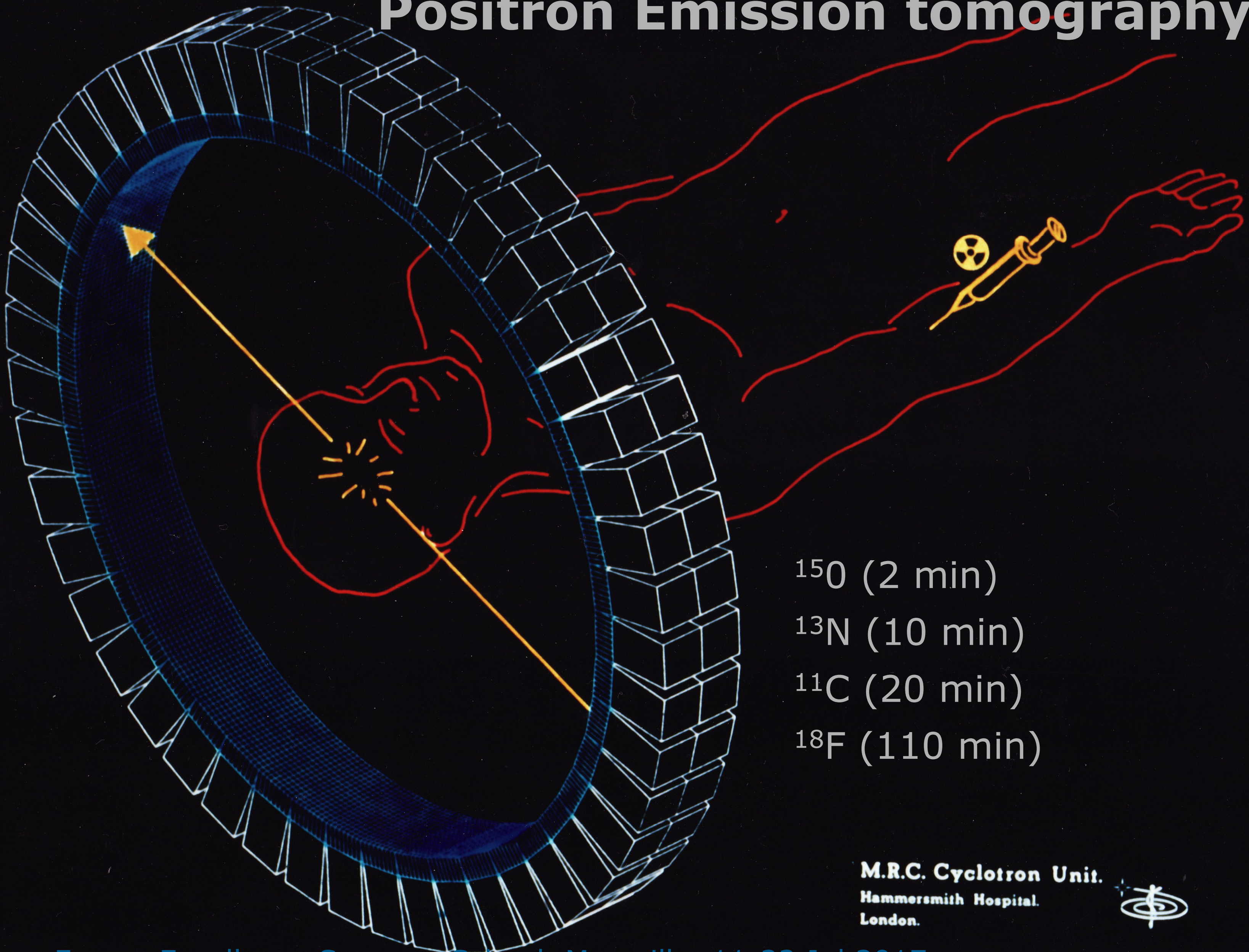

^{15}O (2 min)	511 keV
^{13}N (10 min)	511 keV
^{11}C (20 min)	511 keV
^{18}F (110 min)	511 keV

Anatomy + Function

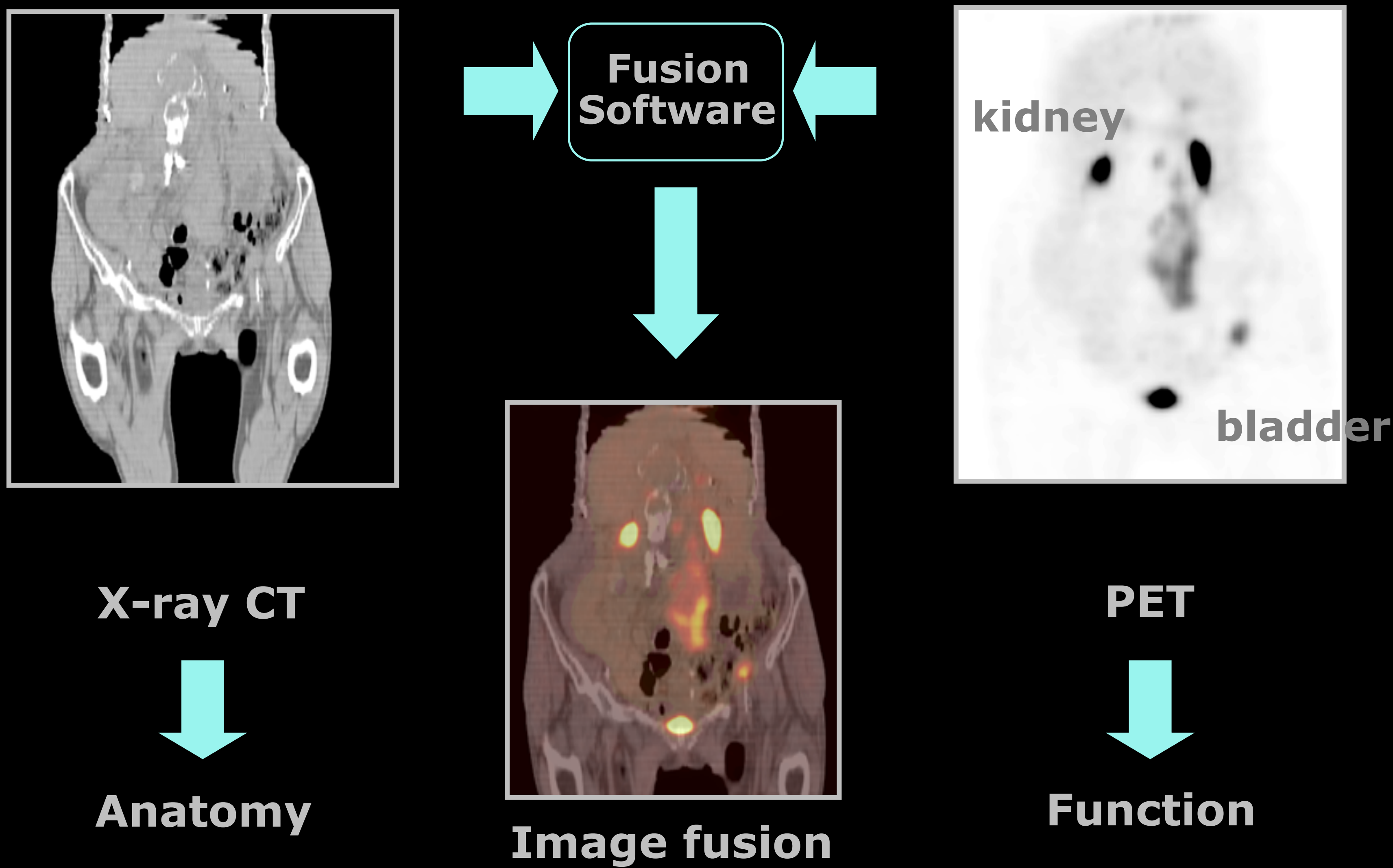

Courtesy: D.W. Townsend, UPMC

1991: PET/CT concept, D.W. Townsend (HUG)

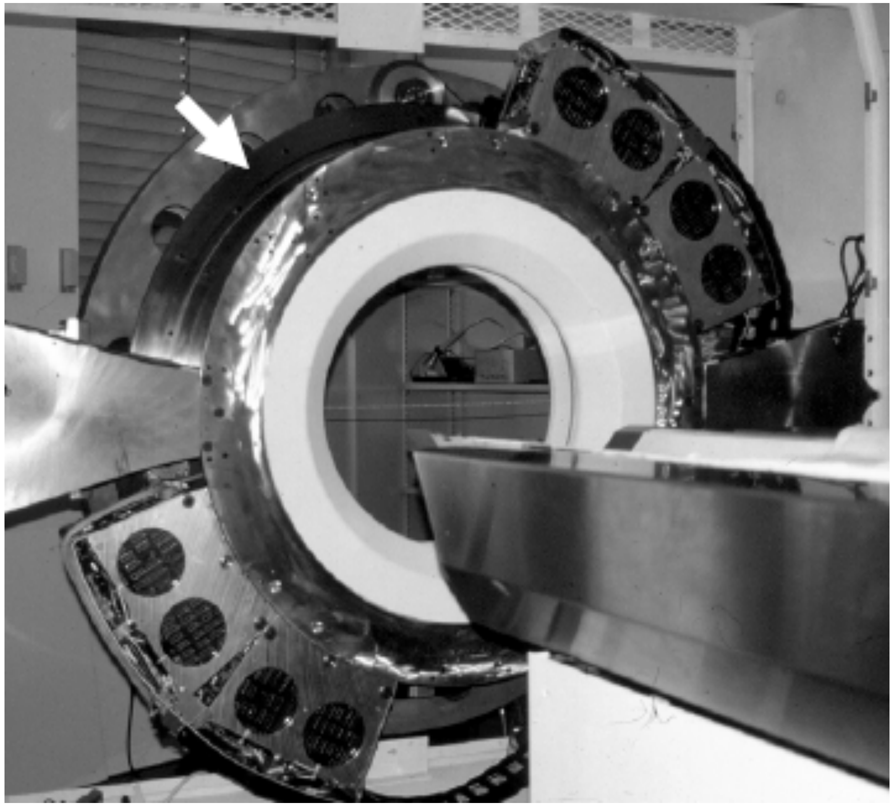

PRT-1

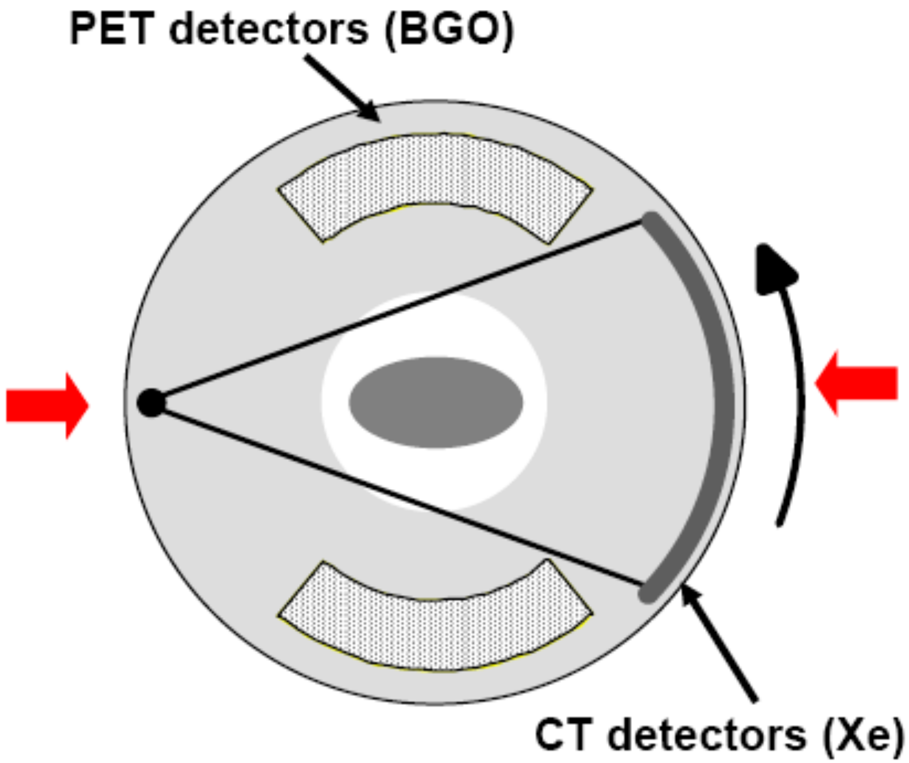

Courtesy: D.W. Townsend, UPMC

CT: 160 mAs; 130 KV_p; pitch 1.6; 5 mm slices

PET: 6.3 mCi FDG; 3 x 10 min; 3.4 mm slices

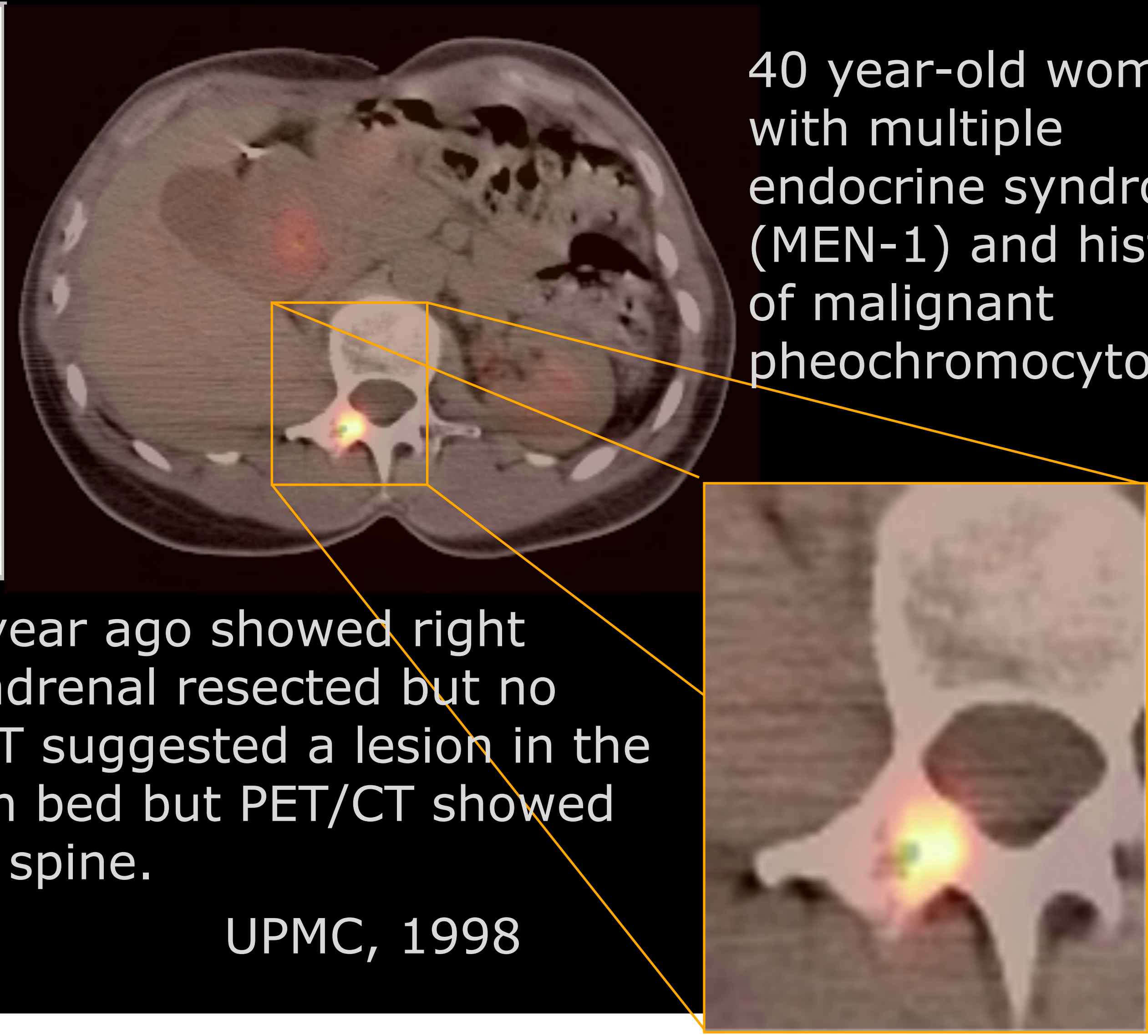

40 year-old woman with multiple endocrine syndrome (MEN-1) and history of malignant pheochromocytoma

MIBG scan one year ago showed right adrenal lesion; adrenal resected but no tumor found. PET suggested a lesion in the adrenal resection bed but PET/CT showed lesion located in spine.

UPMC, 1998

Courtesy: D.W. Townsend, UPMC

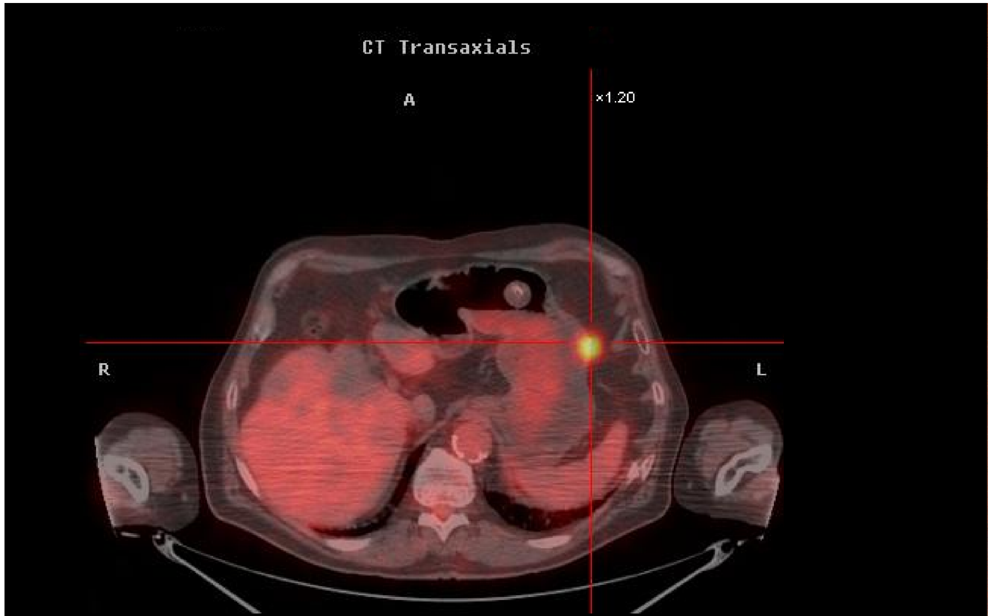

TIME magazine Dec 2000

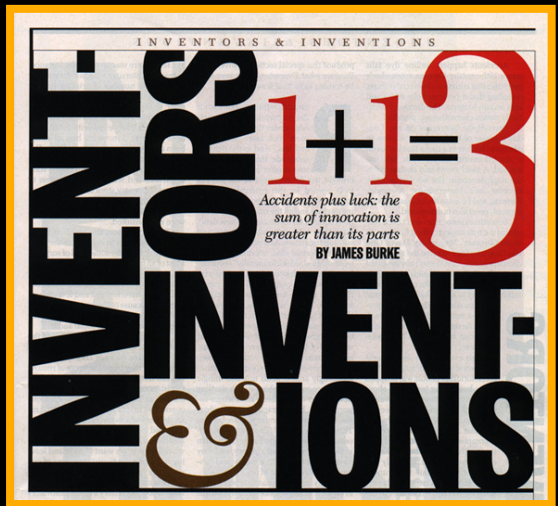

Typical design of a PET/CT scanner

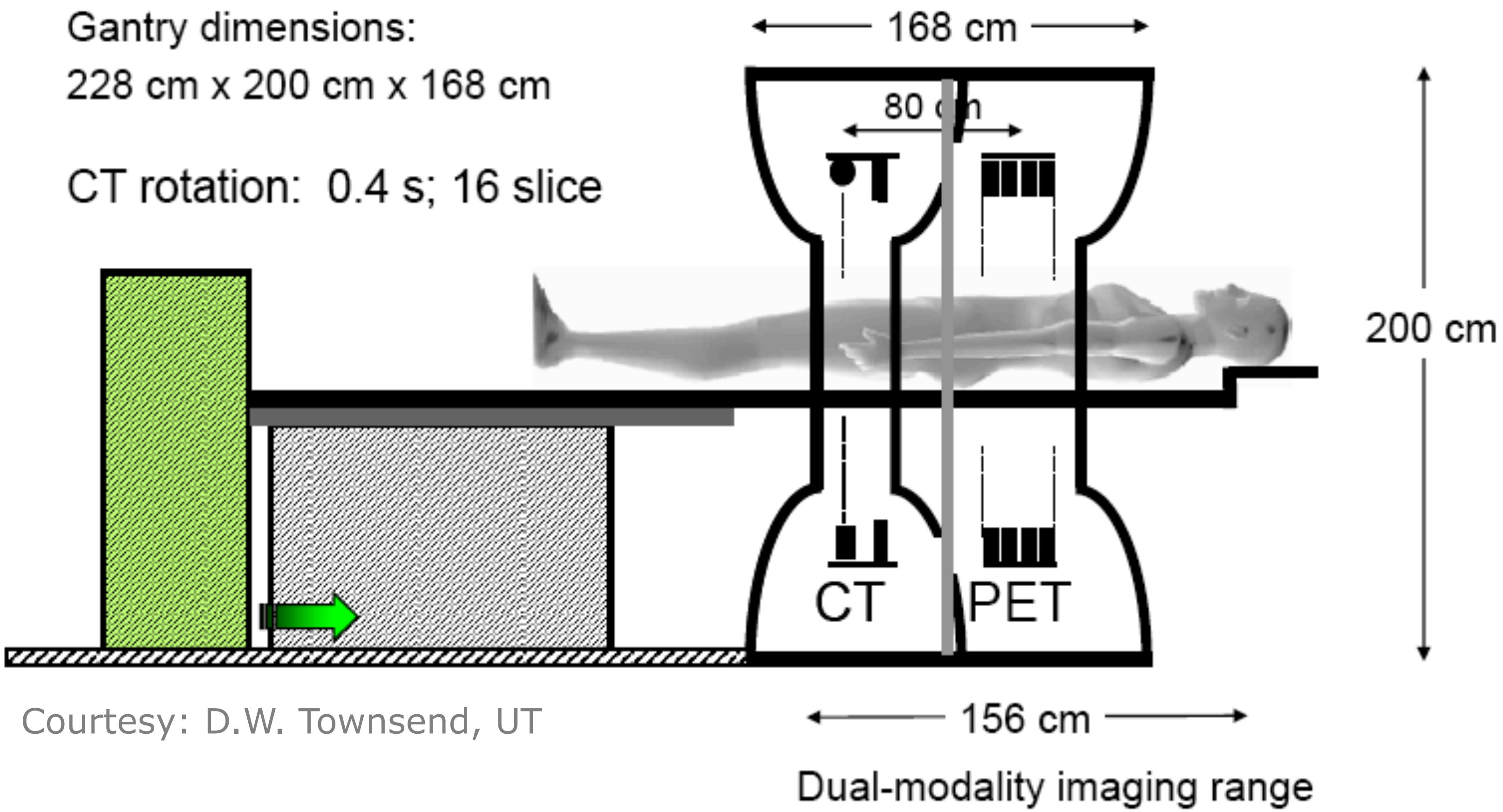

Courtesy: D.W. Townsend, UT

2001 : 1st commercial PET/CT scanner installed in Zurich by GE
2005 : > 650 TEP/TDM scanners installed, 95% PET sales

PET/CT scanners

Discovery IQ, GE

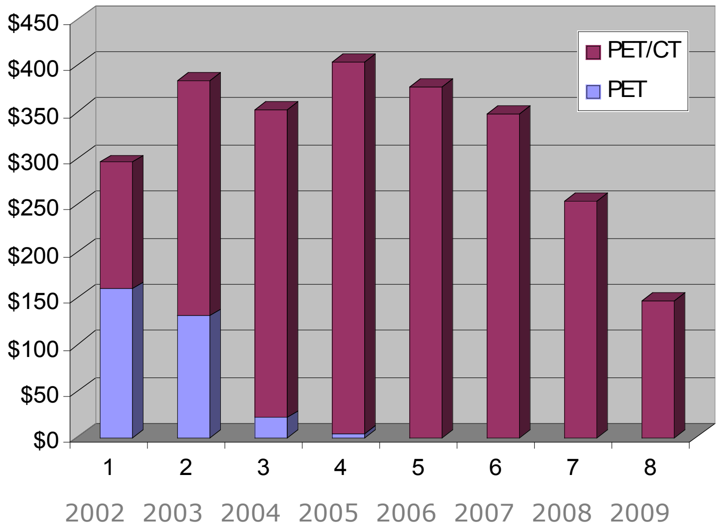

NEMA - US Shipments ($M) TEP/CT

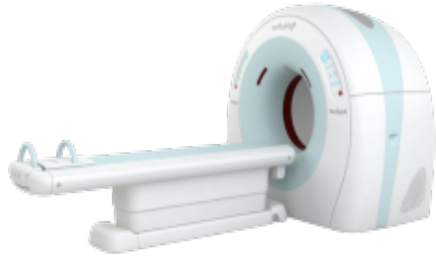

AnyScan, Pozitron Teknik

Courtesy: D.W. Townsend, UT

Gemini, Philips

Celesteion, Toshiba

Biograph, Siemens

uMI 510, United Imaging

SceptreP3, Hitachi

Simultaneous PET/CT: proof of concept with the ClearPET/XPAD prototype

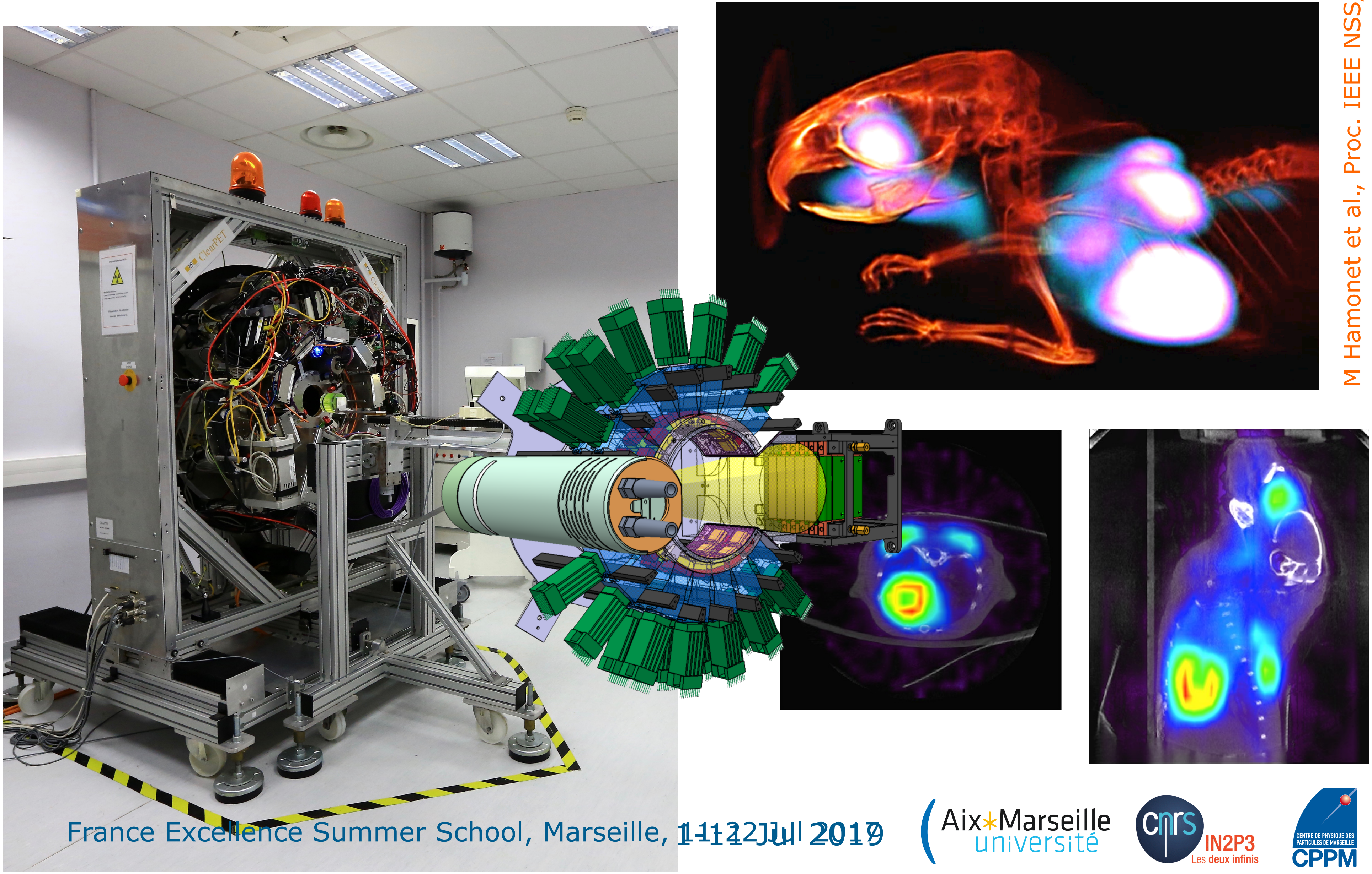

M Hamonet et al., Proc. IEEE NSS/MIC 2016

Patrick Pangaud, Stéphanie Godiot, Mohsine Menouni, Franca Cassol, Mathieu Dupont, Jonathan Graber-Bolis, Loriane Portal, Margaux Hamonet, Amr Habib, Carine Kronland-Martinet, Hamid Ouamara, Didier Benoit, Benoît Chantepie, Rana Khoury, Stanislas Nicol, Yannick Boursier, Jean-Claude Clémens, Thomas Fabiani, Alain Bonissent, Eric Vigeolas, Christophe Meessen, Franck Debarbieux

Frédéric Bompard,
Hector Perez-Ponce,

Stéphanie Hustache,
Arkadisuz Dawiec,
Clément Buton

Nathalie Boudet, Nils Blanc,
Jean-François Bérar

ITMOs Technologie
pour la Santé et Cancer,
France Life Imaging

CERN Crystal Clear Collaboration